Multi-scale/signal Seismic imaging of Fault Zone Environments

Yehuda Ben-Zion, University of Southern California
with D. Zigone, Z. Ross, A. Allam, H. Qui, P. Share, F. Vernon, G. Hillers, M. Campillo, P. Roux & others

Complex hierarchical structures with:

•Strong geometrical and material heterogeneities

•Strong attenuation

•Nonlinear propagation effects

•Many scales and secondary structures: interfaces (bimaterial), damage zones, basins, branching faults, heterogeneous bounding blocks, etc.

Very challenging targets for detailed imaging

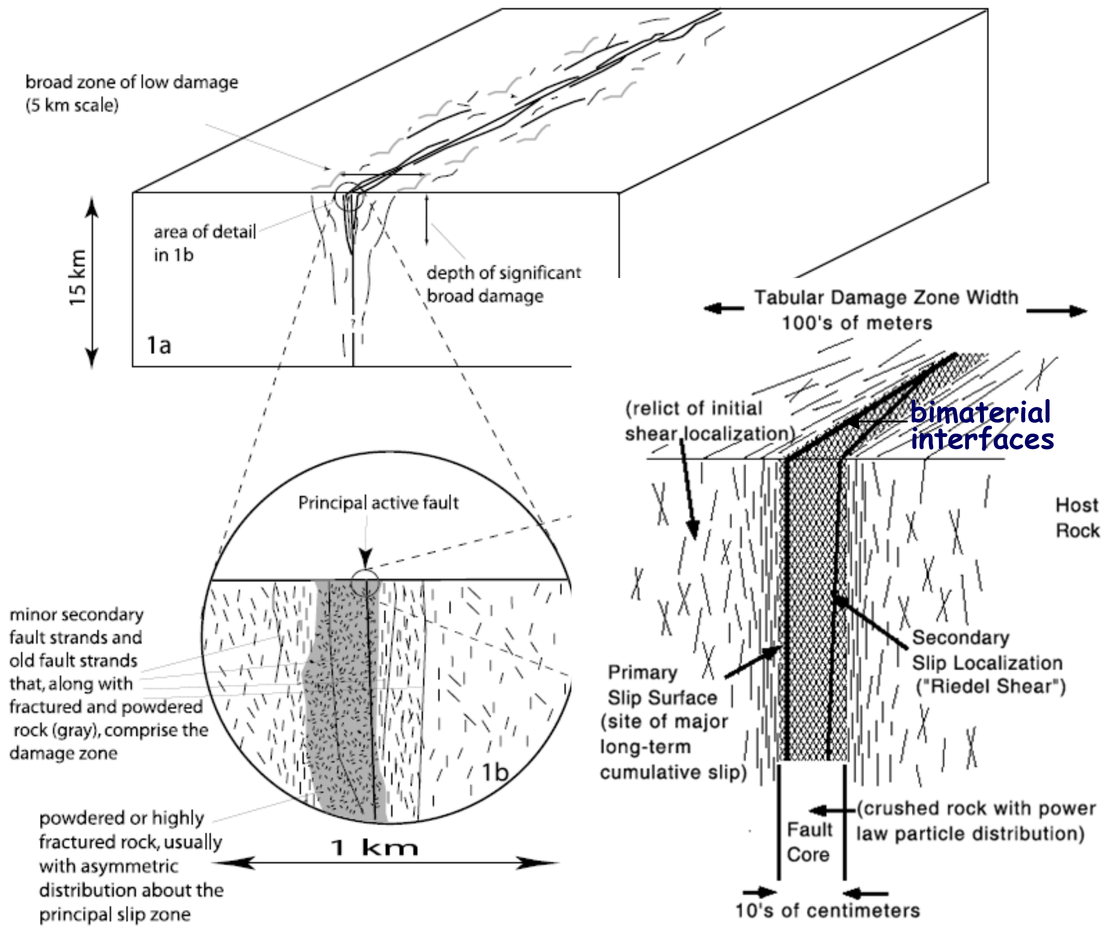

Ben-Zion and Sammis (2003)
Rockwell and Ben-Zion (2007)

Multi-scale/signal Seismic imaging of Fault Zone Environments

Yehuda Ben-Zion, University of Southern California
with D. Zigone, Z. Ross, A. Allam, H. Qui, P. Share, F. Vernon, G. Hillers, M. Campillo, P. Roux & others

Why image fault zones?

- Derivation of earthquake source properties.
- Evolutionary processes on long (tectonic) and short (e.g., precursory) timescales.
- Static/dynamic stress fields (e.g. from internal structure).
- Brittle rock rheology (e.g. from observing & monitoring rock damage).
- Elements of FZ structure (bimaterial interfaces and damage zones) can control future (and reflect past) earthquake rupture properties.

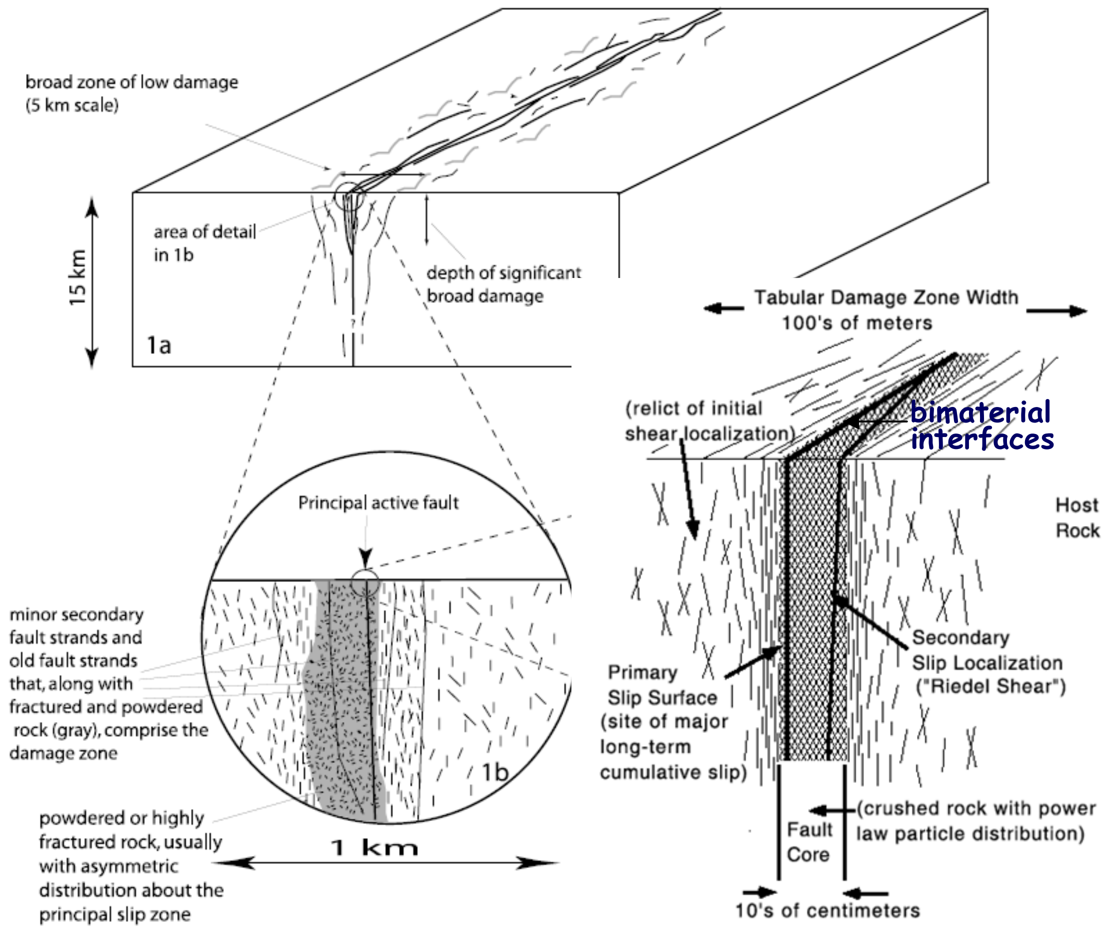

Ben-Zion and Sammis (2003)
Rockwell and Ben-Zion (2007)

Multi-scale/signal Seismic imaging of Fault Zone Environments

Yehuda Ben-Zion, University of Southern California
with D. Zigone, Z. Ross, A. Allam, H. Qui, P. Share, F. Vernon, G. Hillers, M. Campillo, P. Roux & others

Why image fault zones?

- Derivation of earthquake source properties.
- Evolutionary processes on long (tectonic) and short (e.g., precursory) timescales.
- Static/dynamic stress fields (e.g. from internal structure).
- Brittle rock rheology (e.g. fron observing & monitoring rock damage).
- Elements of FZ structure (bimaterial interfaces and damage zones) can control future (and reflect past) earthquake rupture properties
- FZs control crustal fluid flow: hydrology, oil, sub-surface storage, minerals, etc.

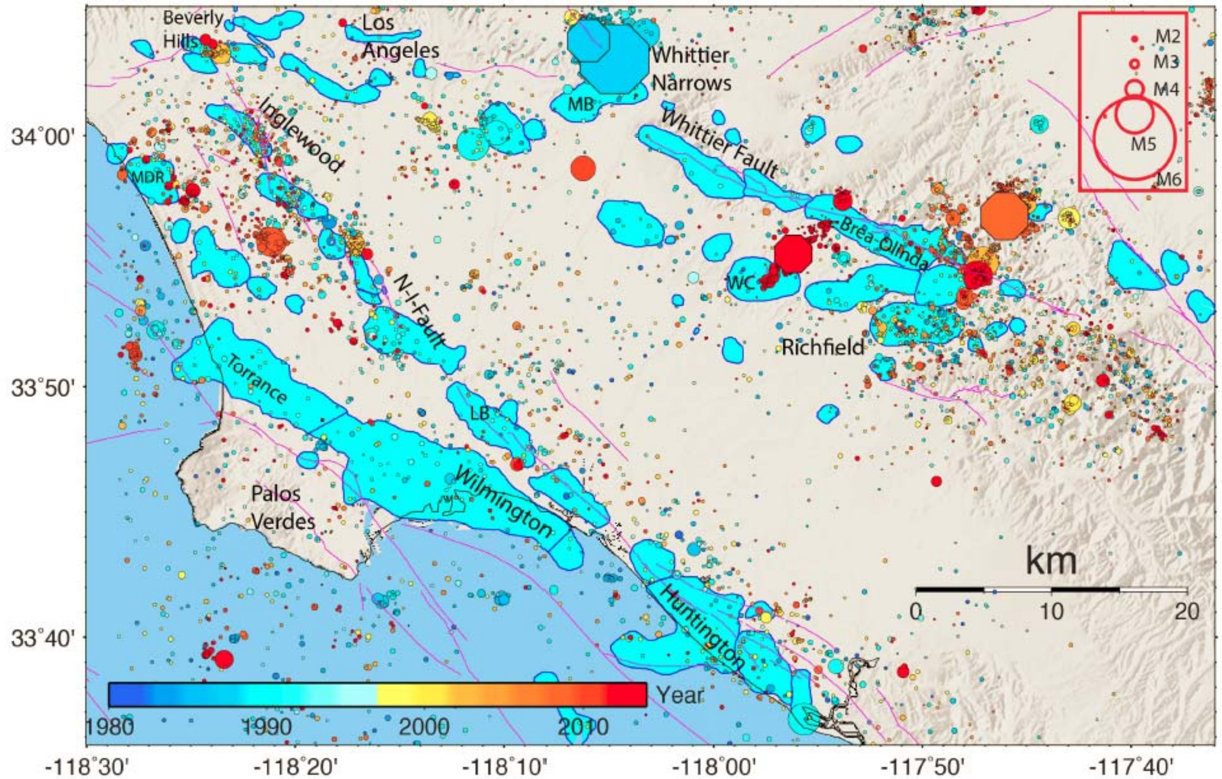

Hauksson et al. (2015)

Focus in this talk: The San Jacinto Fault Zone in southern CA

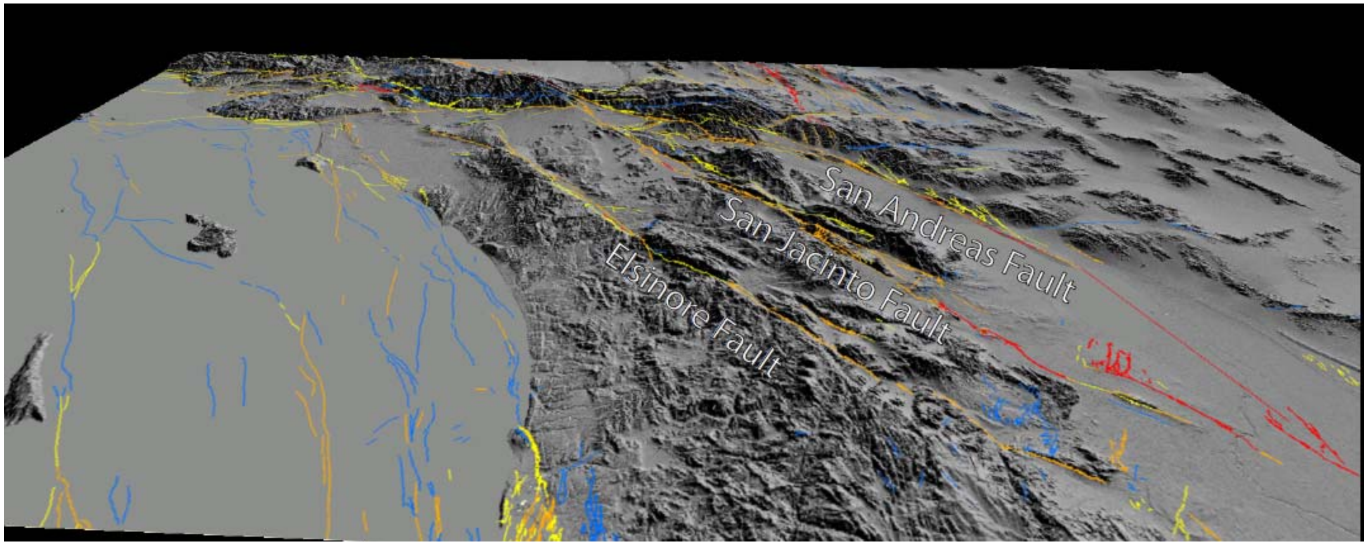

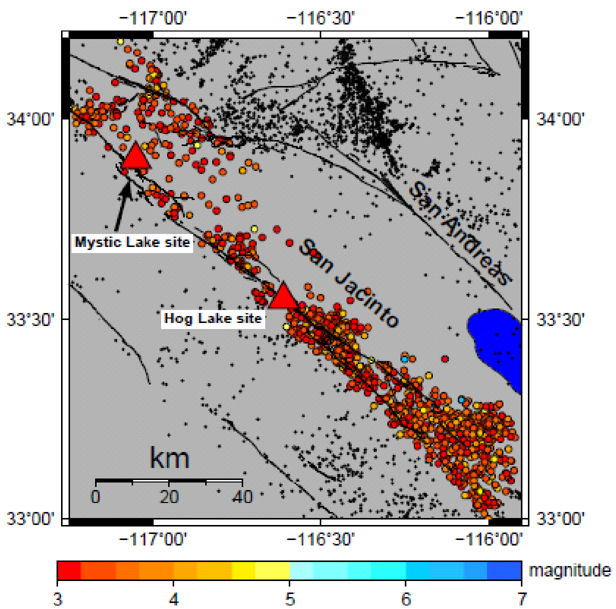

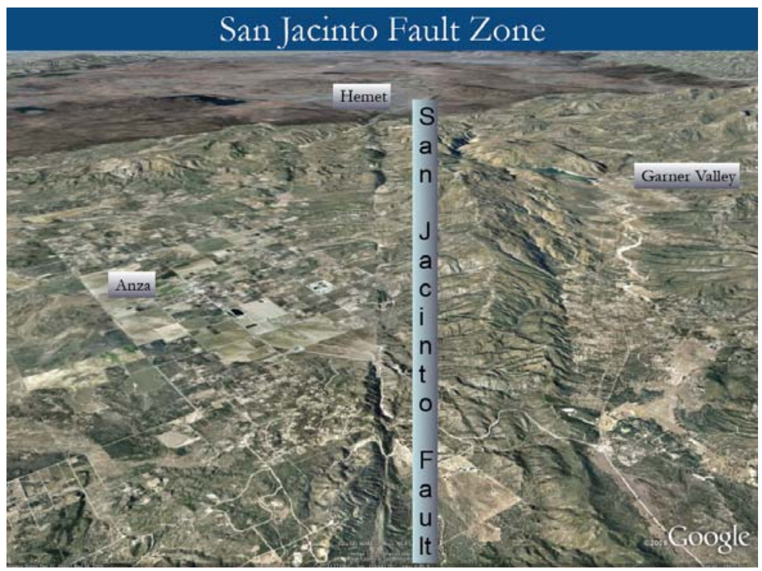

Hierarchical Seismic Networks around the San Jacinto Fault Zone in southern CA

Data: Earthquake waveforms, ambient seismic noise (+ small "Besty" gunshots)

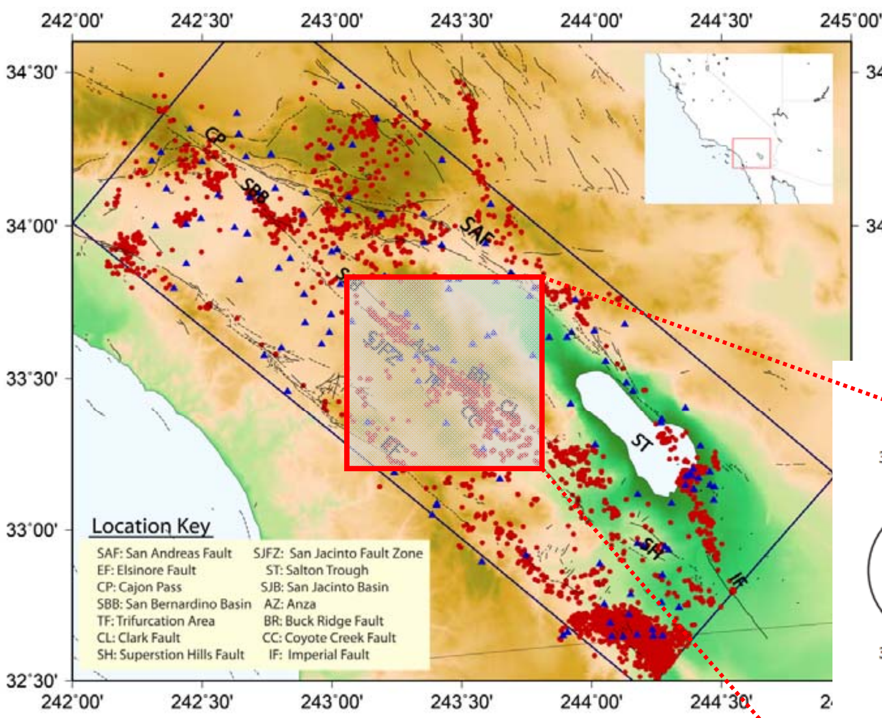

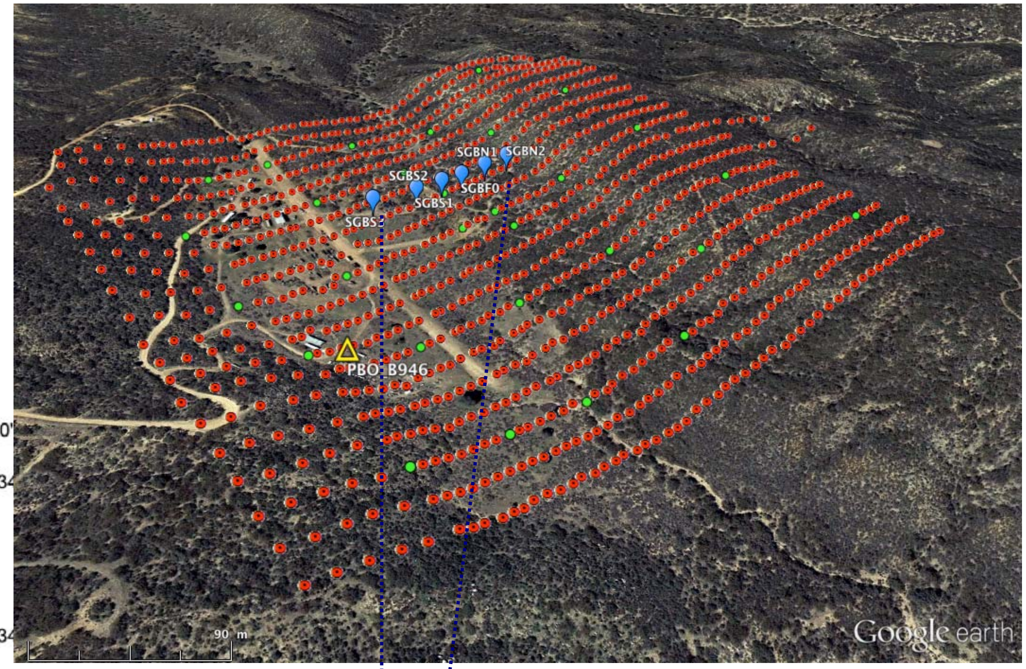

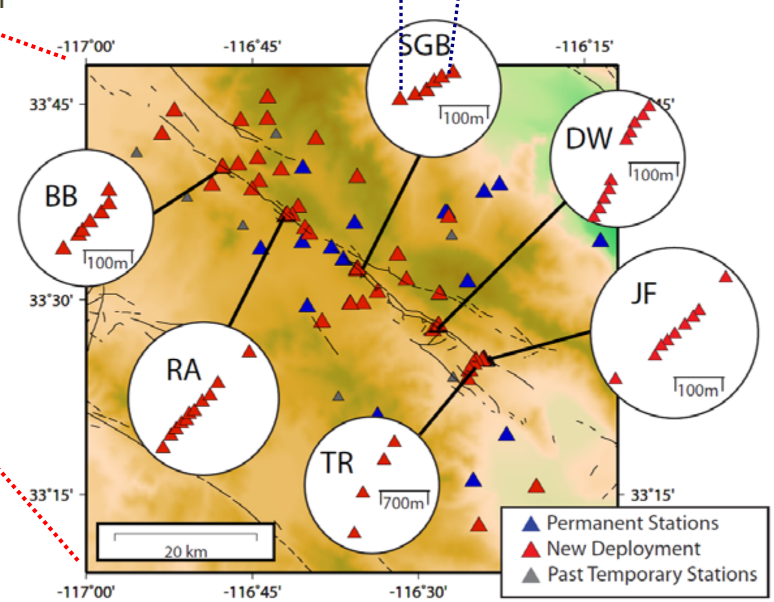

Signals: P & S body waves, Rayleigh & Love surface waves,
Fault zone head & trapped waves
(+ anisotropy and attenuation)

Seismic Velocity Structures in the Southern California Plate Boundary Environment from Double-difference Earthquake Tomography (Allam and Ben-Zion, GJI, 2012)

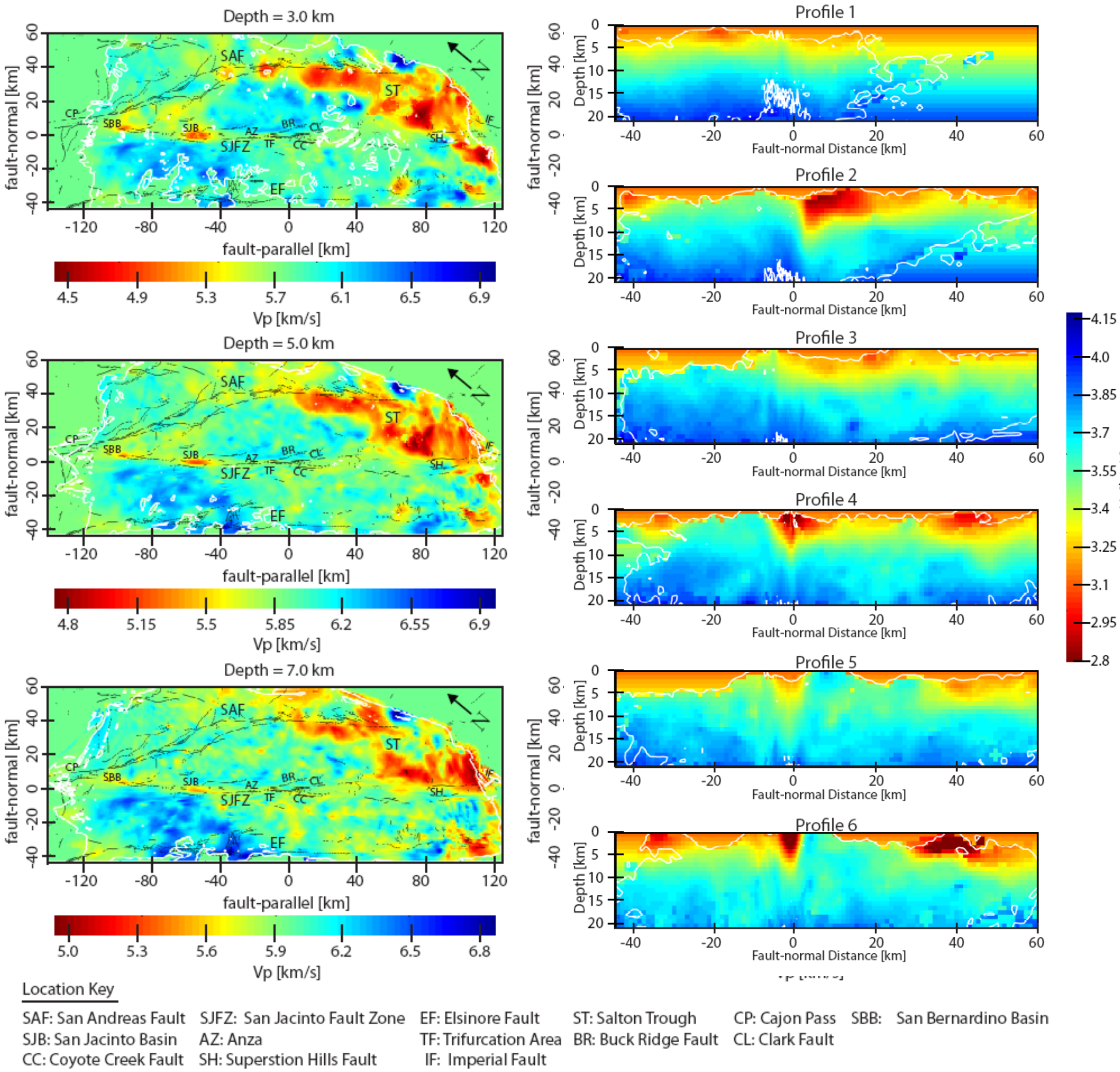

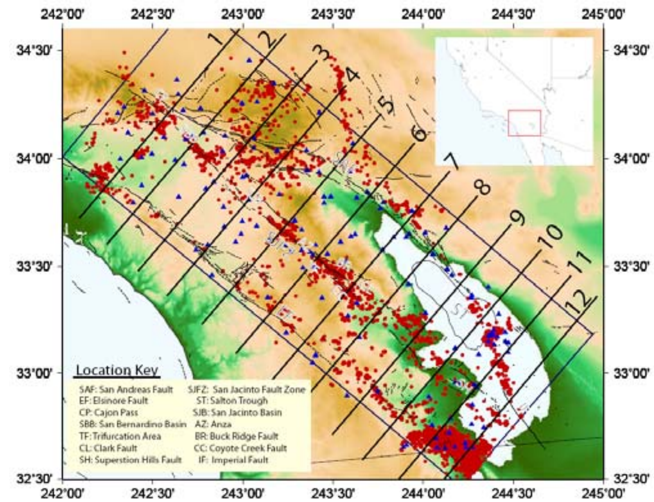

Horizontal resolution 2-3 km over depth section 2-15 km

Broad low velocity fault zone layers (3-6 km wide) are:

-Seen clearly along the SJFZ

-Offset to the NW in the central section

-Prominent generally in top 5 km

-Follow overall "flower" shape with depth

-Larger reductions of Vs (up to 40% in top 3-5 km) than Vp

Clear velocity contrasts (bimaterial interfaces?) in different sections; polarity flips NW of SJB.

Additional detailed results on complex SJFZ regions given by Allam, Ben-Zion, Kurzon, Vernon (GJI, 2014)

Noise-based Imaging of Southern California Plate Boundary Area

Dimitri Zigone, Yehuda Ben-Zion, Michel Campillo, Phillipe Roux (2015)

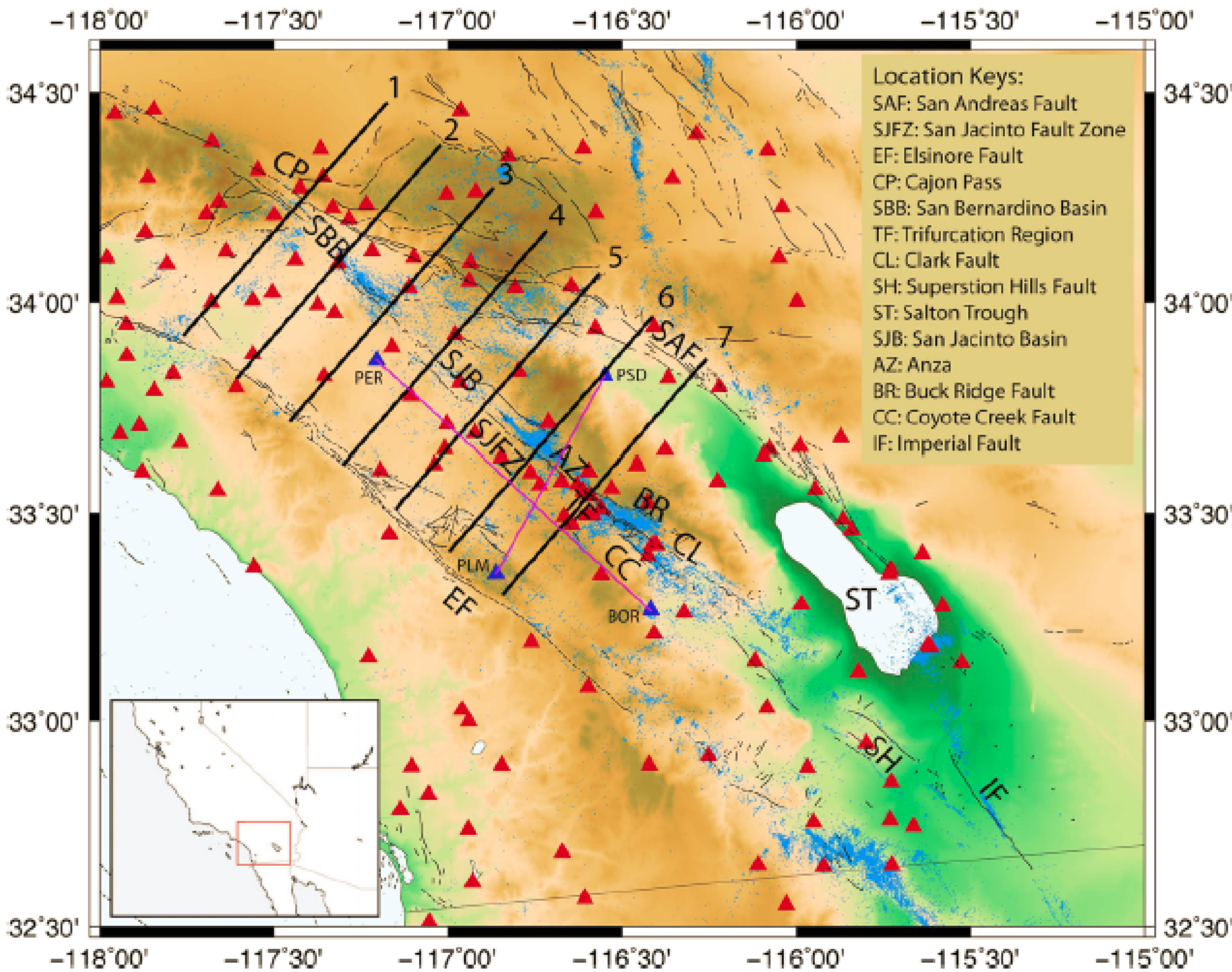

158 Stations

Ambient seismsic noise in 2012 up to 1 Hz

Three components boradband (66%) and short period (33%) sensors

Cross-correlations : processing

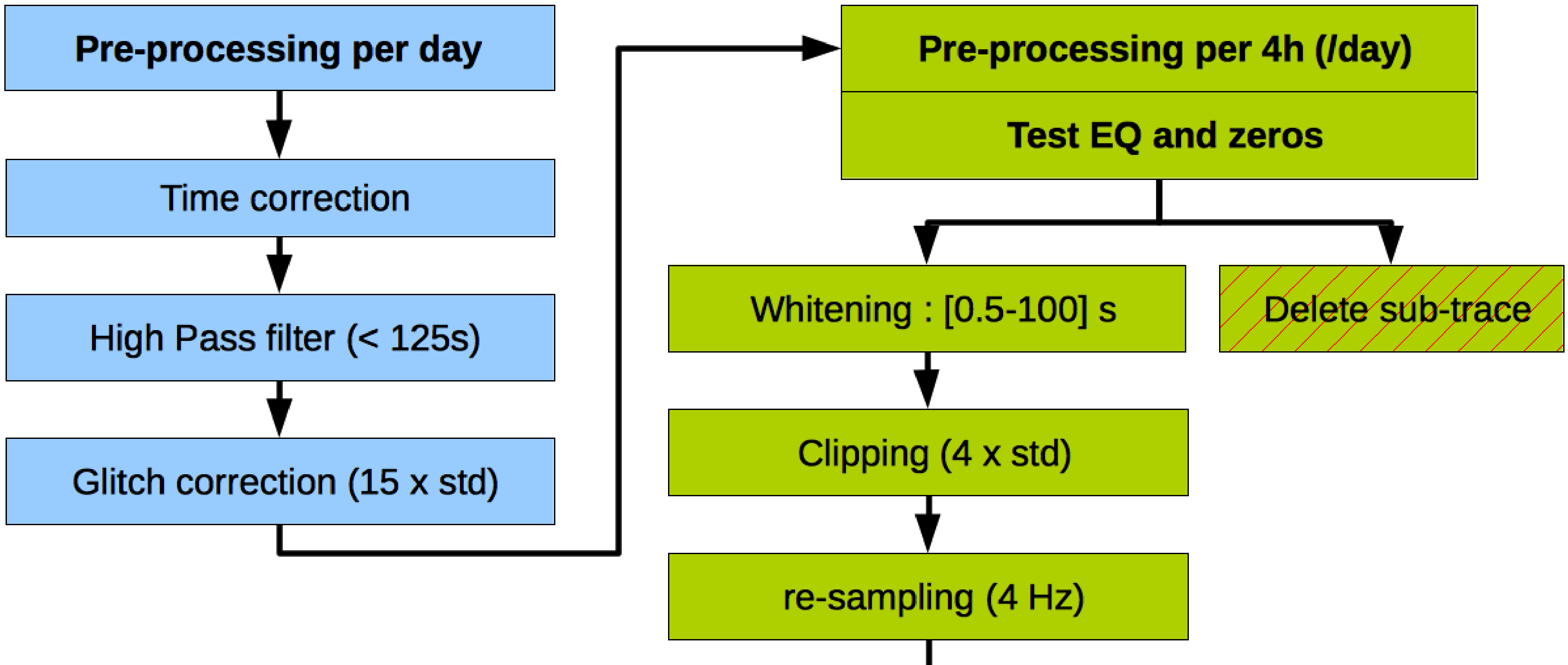

(Bensen et al. , 2007 ; Groos et al. ,2010)

Correlations per 4h (stacked per day)

9 components
Maxlag = 300 s

$$[C_{AB}(t)]_{ij} = \frac{\int_0^T S_{A,i}(\tau)\, S_{B,j}(t+\tau)\,d\tau}{\sqrt{\int_0^T S_{A,i}^2(\tau)\,d\tau \int_0^T S_{B,j}^2(\tau)\,d\tau}}$$

Surface Waves Green's functions and Velocity Measurements

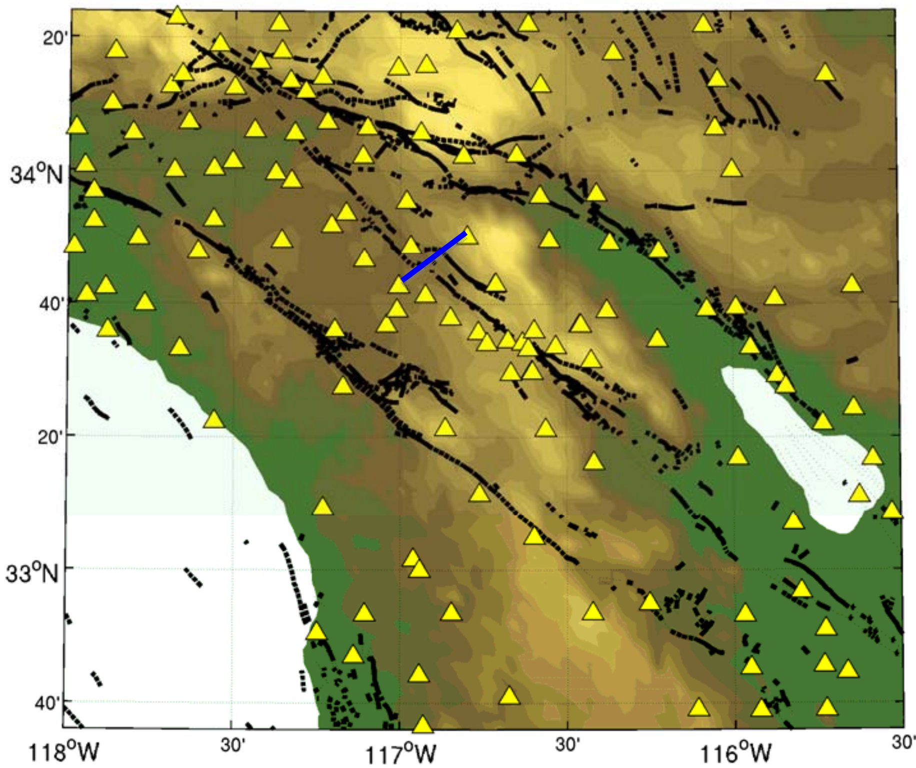

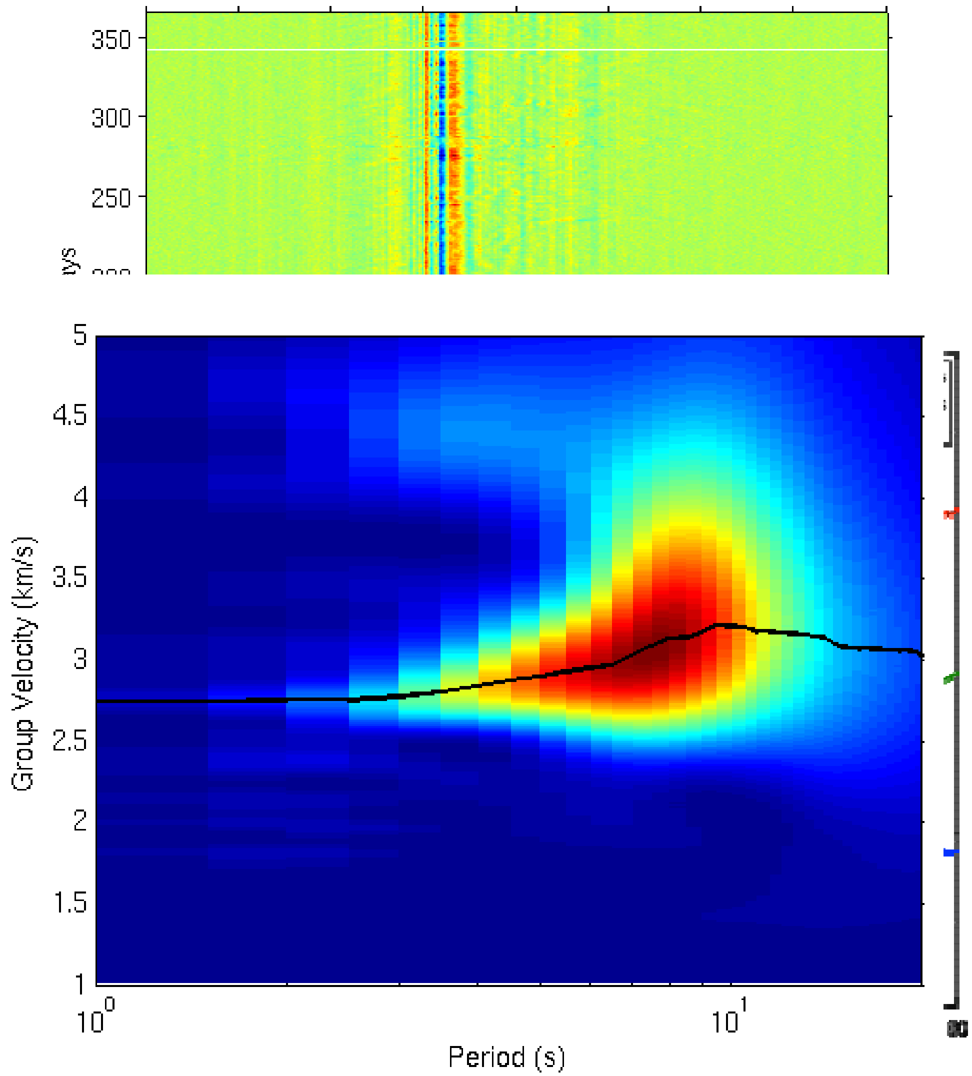

Frequency time analysis (Levshin et al, 1989)

Asymmetric correlogram with clear dispersive surface waves

Perform frequency-time dispersion analysis (Levshin et al, 1989)

Use of the correlation tensor

- Rayleigh wave:
  - Frequency-time analysis of ZZ, RR, ZR, RZ on both the causal and acausal parts; 8 possible measurements
  - Multiply the results
  - Make dispersion measurements
- Love wave:
  - Uses of TT causal and acausal.
  - Only two measurements

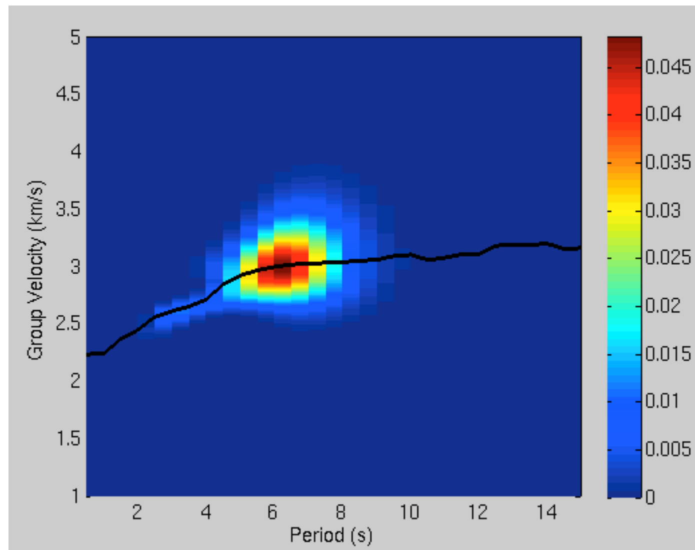

Frequency-time dispersion analysis (Levshin et al, 1989)

Propagation of Rayleigh and Love waves

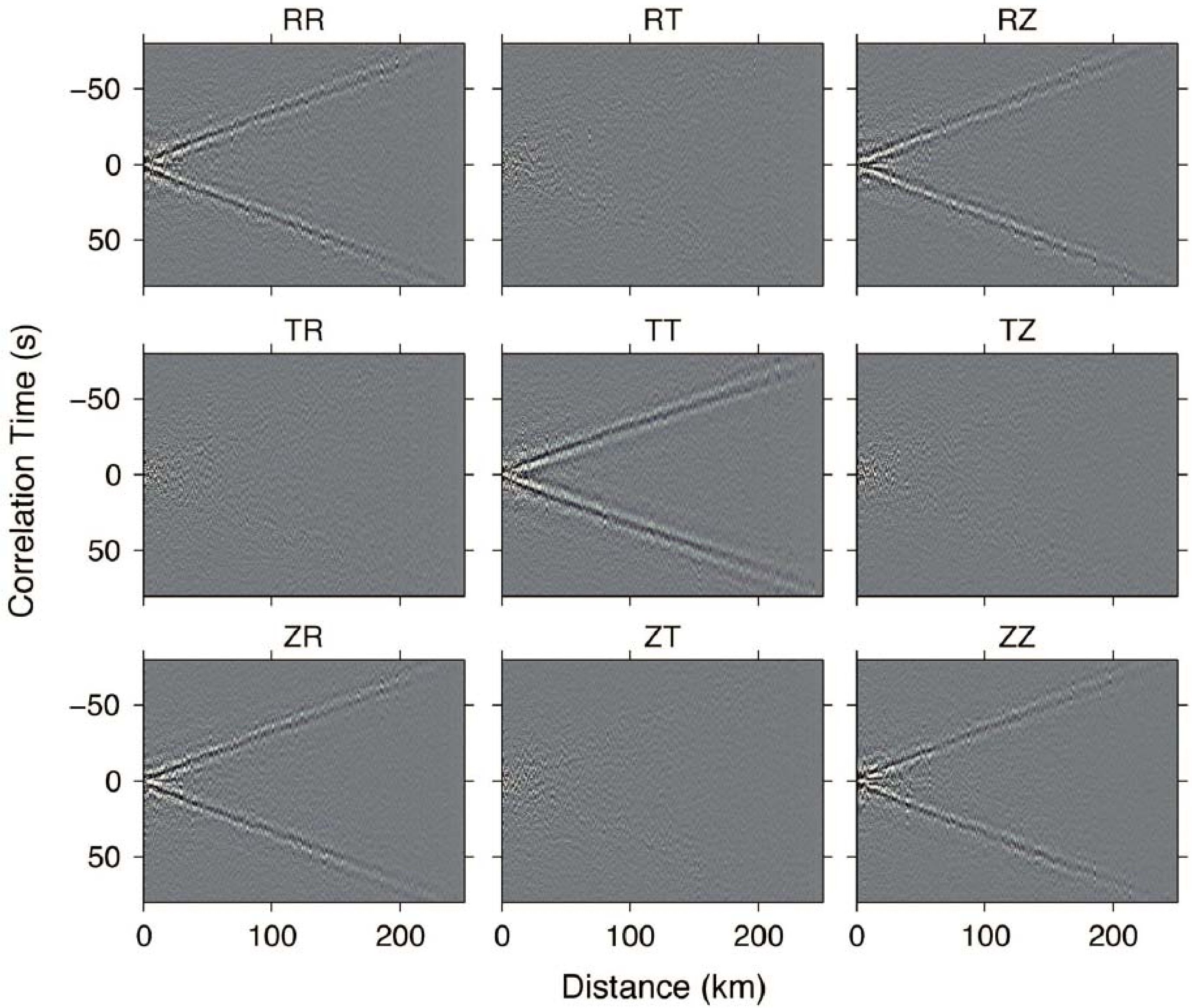

Group Velocity Maps

- Inversion of velocity from dispersion curves (Barmin et al. 2001).
- 1.5 km grid ; use only cells with >3 measurements

Number of paths per cell (used as weight in the inversion)

7 sec Rayliegh wave

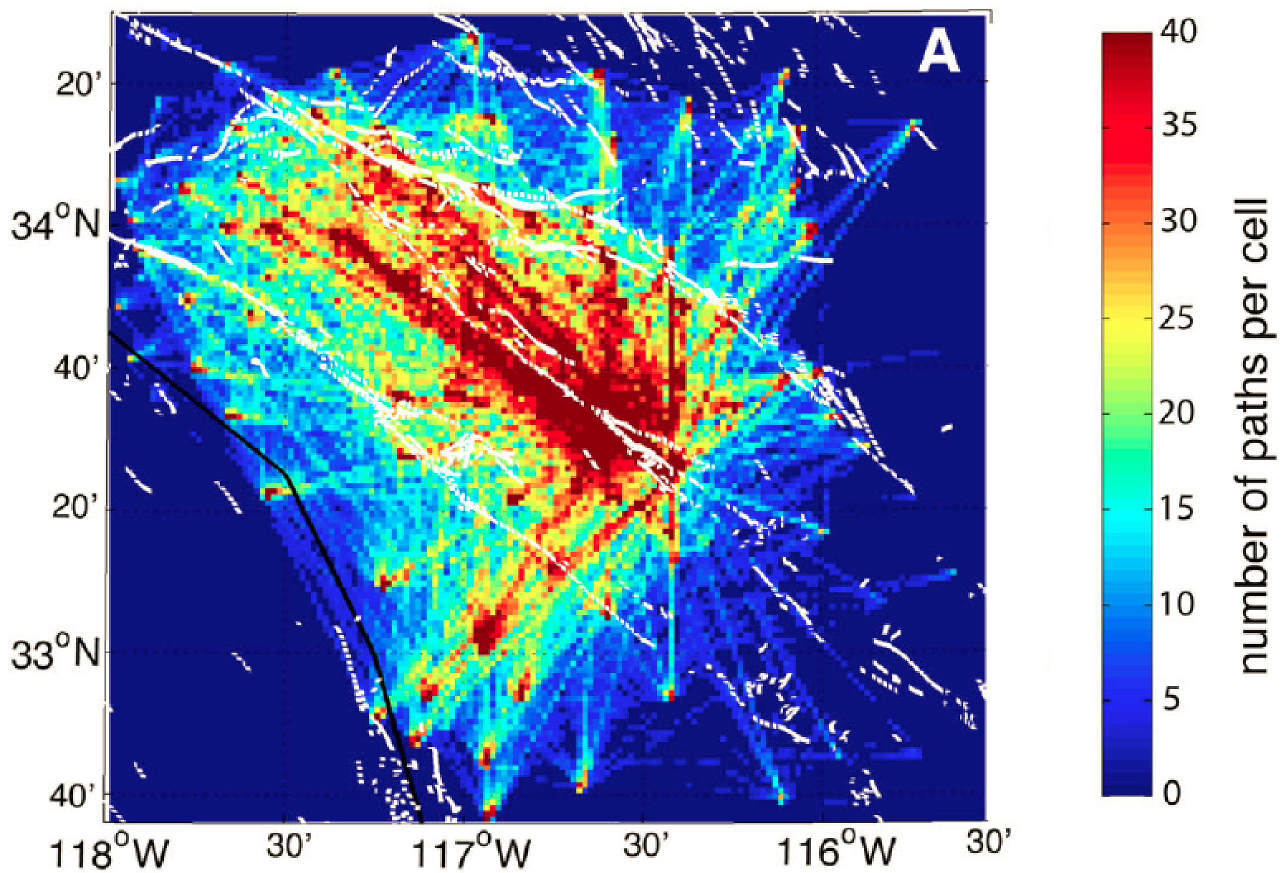

Rayleigh

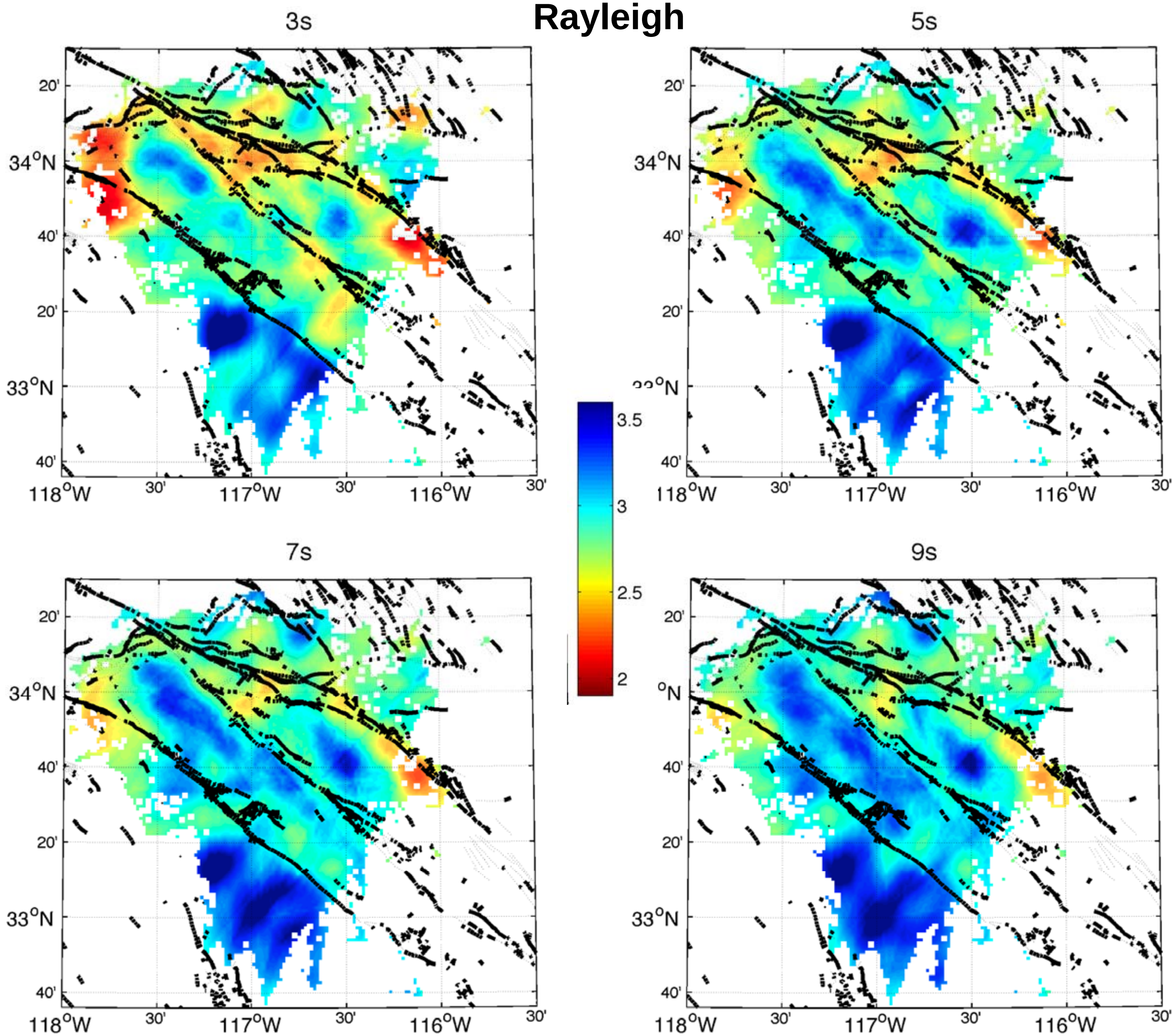

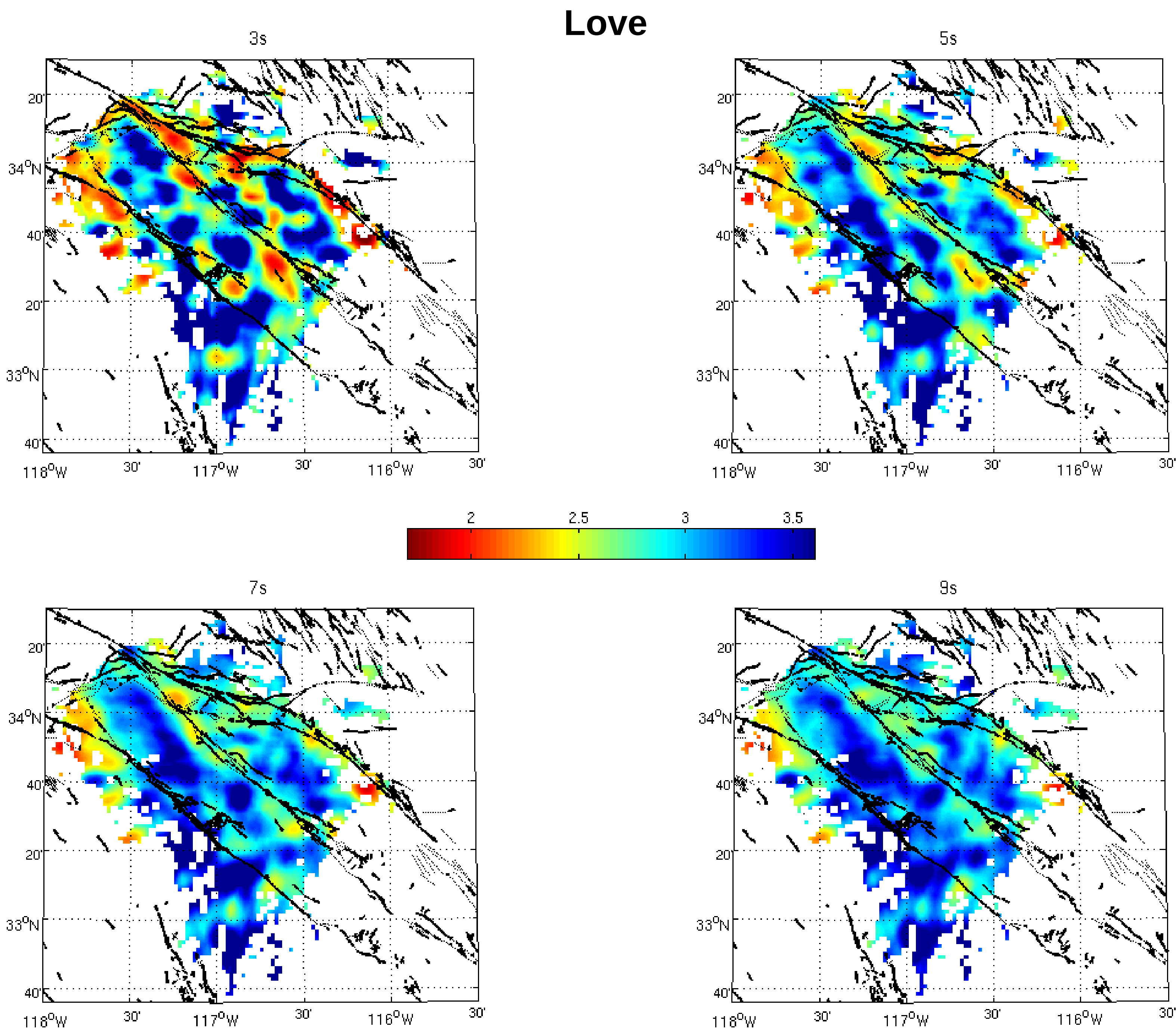
Love
3s
5s
7s
9s
2
2.5
3
3.5
20'
34°N
40'
20'
33°N
40'
118°W
30'
117°W
30'
116°W
30'

Vs Maps (linearized Inversion of Hermann and Ammon, 2002)

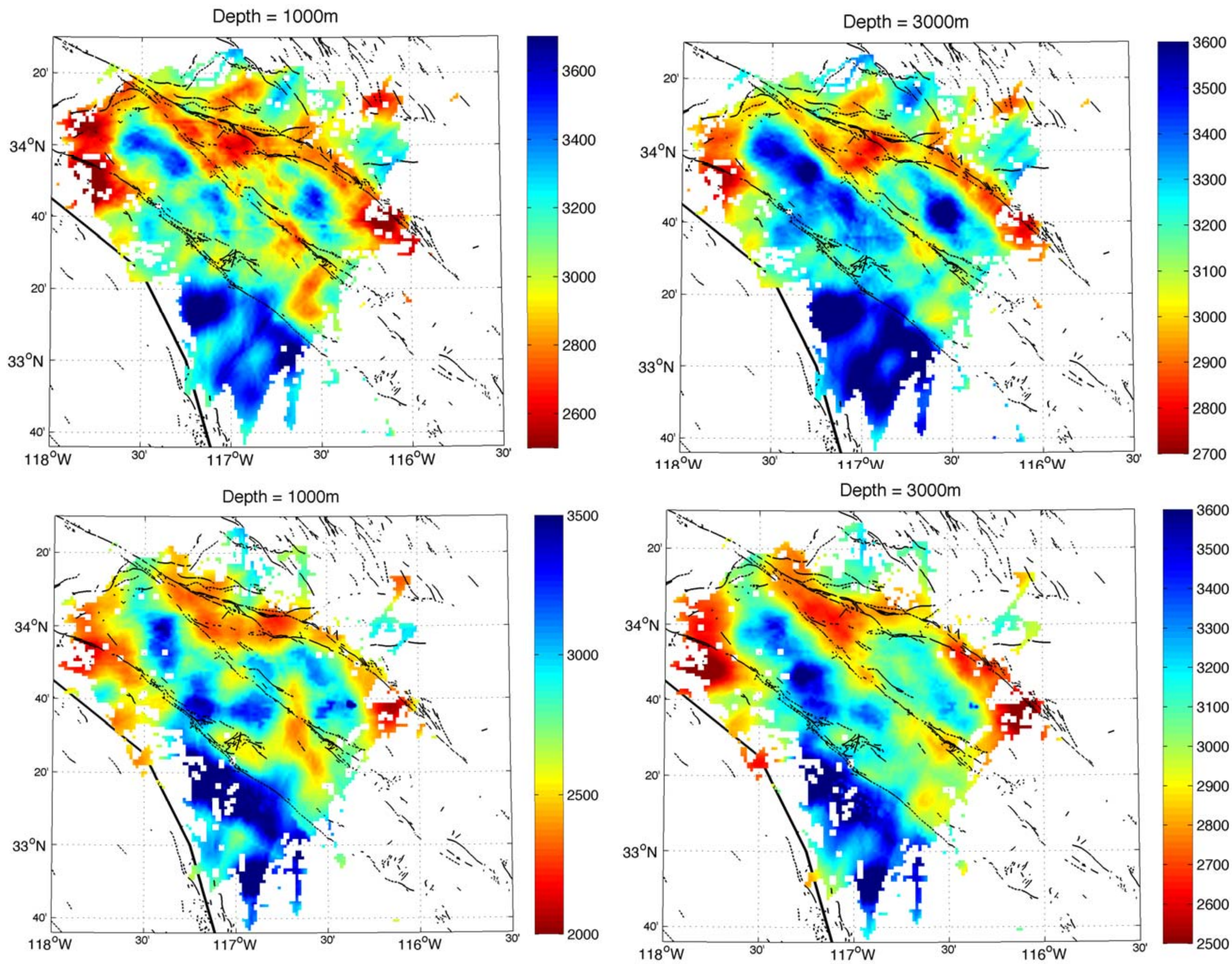

From Rayleigh waves

From Love waves

Vs from Rayleigh waves

Horizontal resolution 2-3 km over depth section 1-7 km

Broad low velocity fault zone layers (3-6 km wide)

Clear velocity contrasts in different sections; the polarity flips NW of SJB.

2-θ anisotropy with fast directions parallel to simple fault sections and random in complex areas

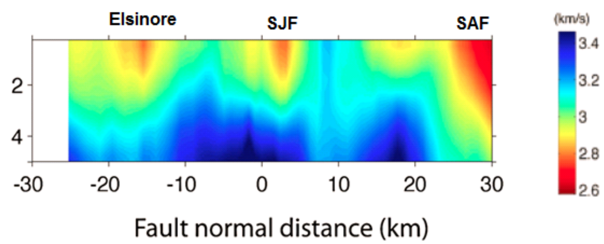

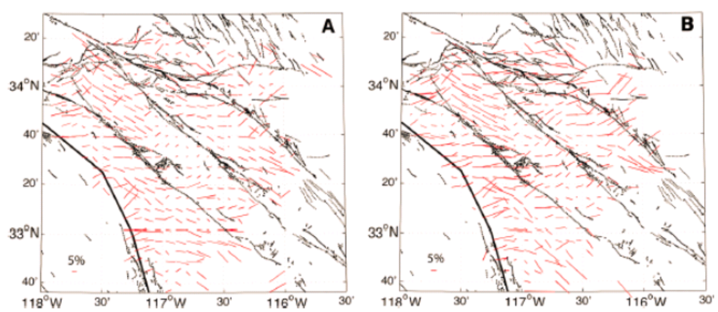

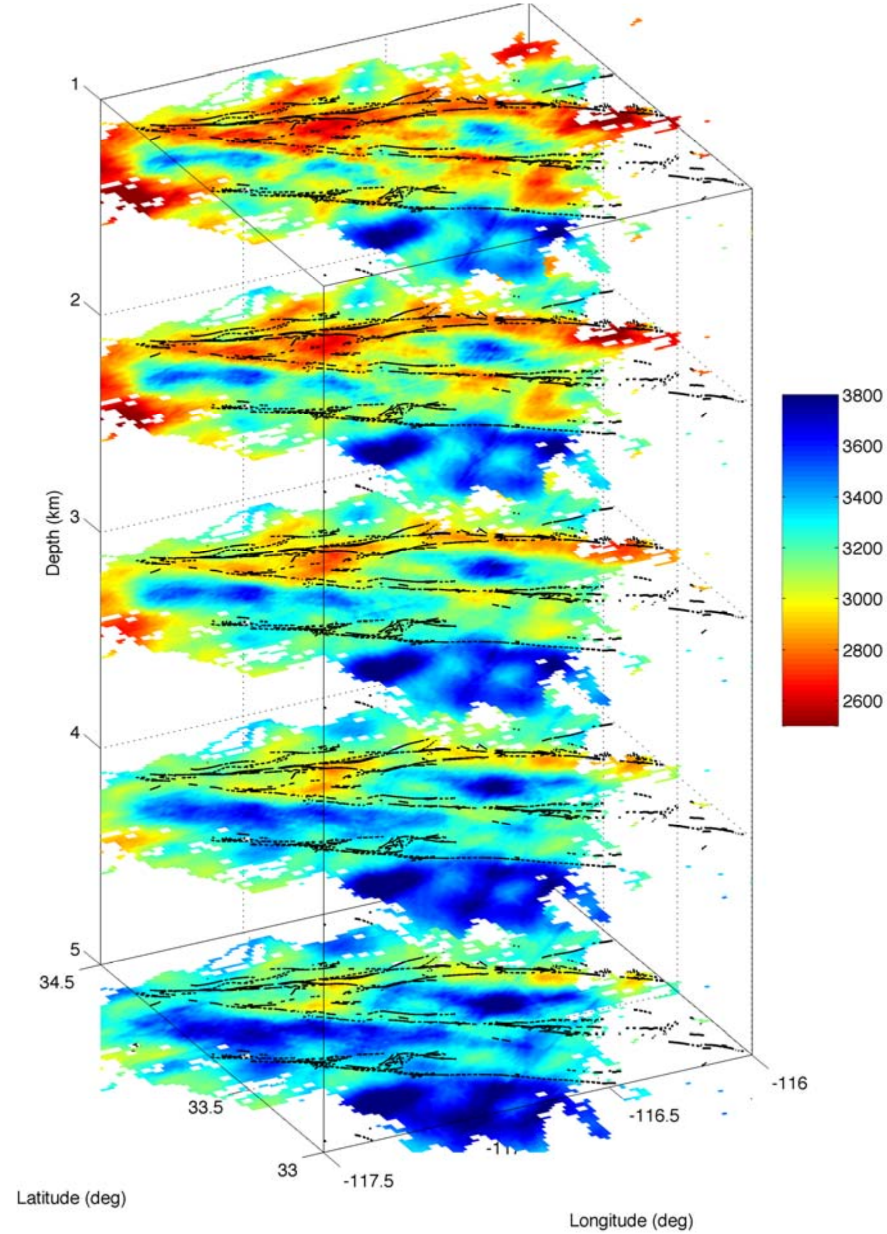

Summary of "large scale" earthquake- and noise-based imaging results

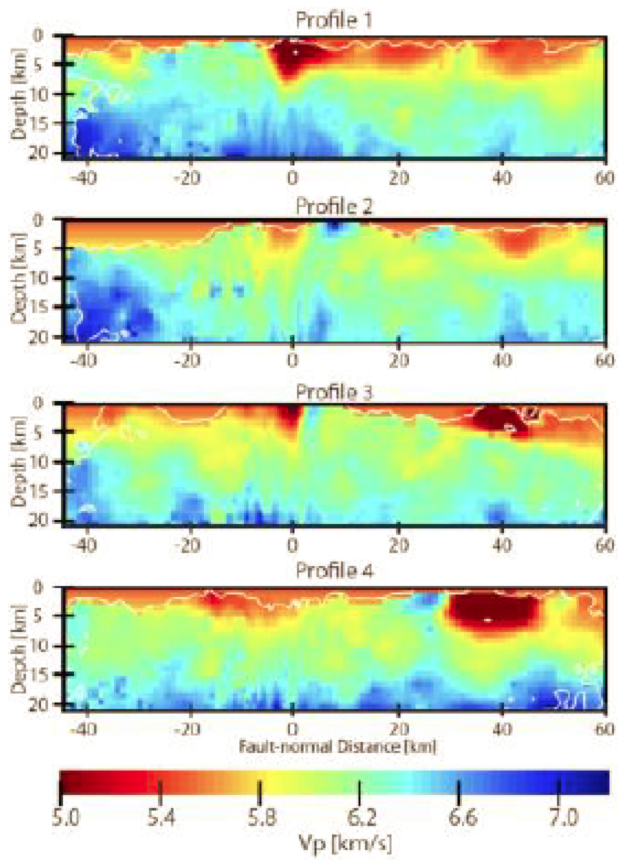

Vp TomoDD results
(Allam & Ben-Zion 2012)

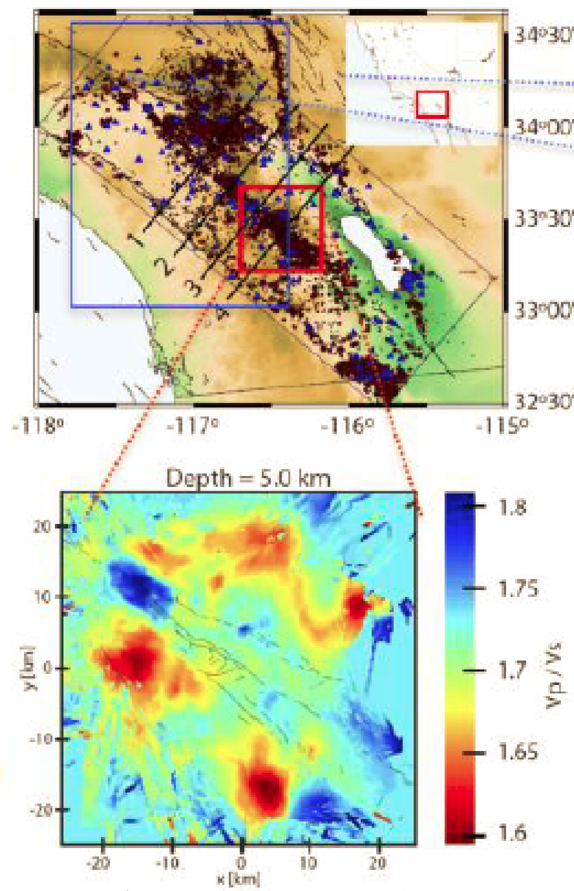

Vp/Vs TomoDD results
(Allam et al. 2014)

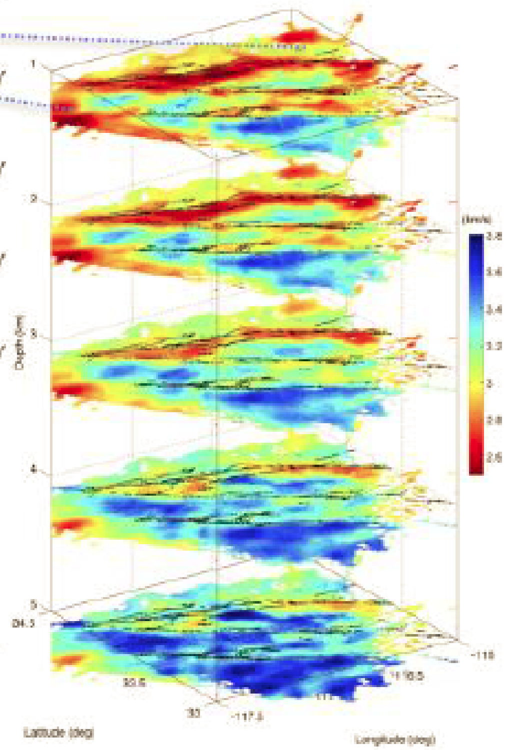

Composite noise-based 3D results (Zigone et al. 2015)

The TomoDD and Noise-based images resolve multiple important structural features of the plate boundary region around the SJFZ with horizontal scale of 2-3 km over the depth section 0.5-15 km.

Internal components of the SJFZ are imaged with fault zone head and trapped waves (next slides).

The structure in the top 0.5 km is imaged (up to the surface) with high-frequency noise (1-200 Hz). (following slides).

Fault zone head and trapped waves

Ben-Zion, 1989, 1990

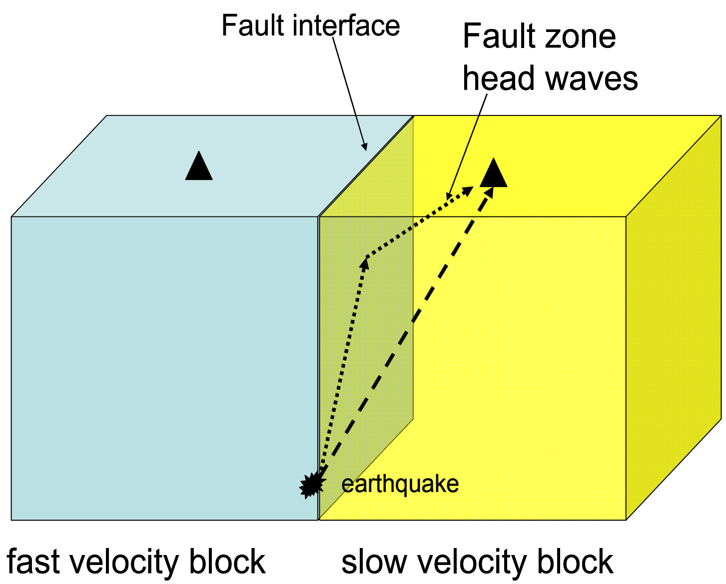

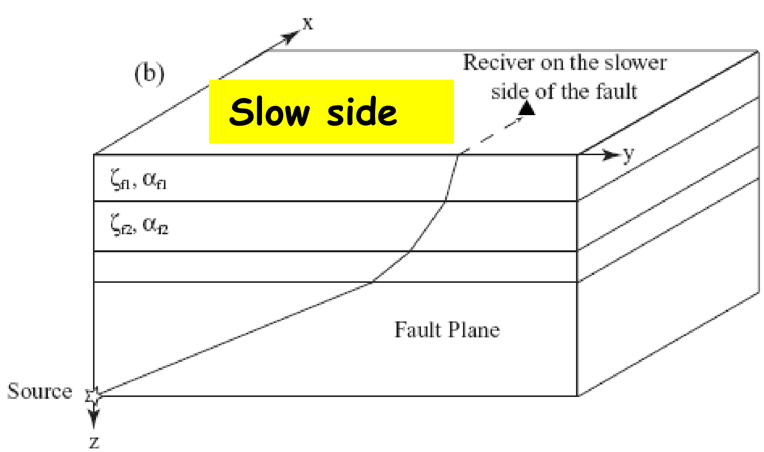

Ben-Zion and Aki, 1990

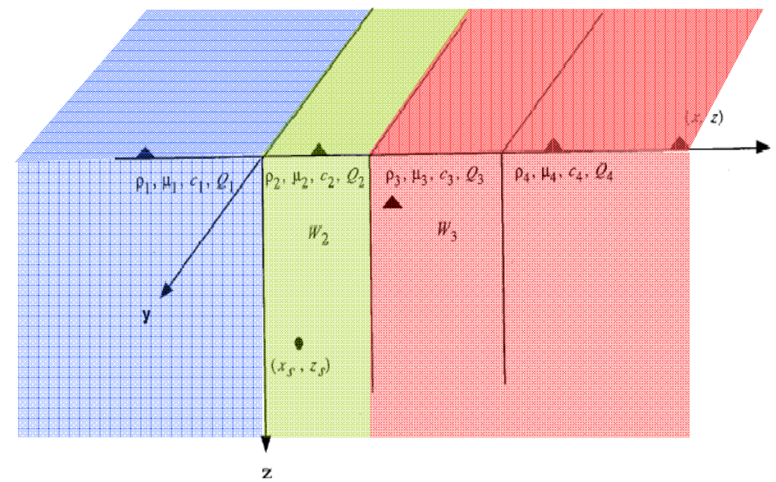

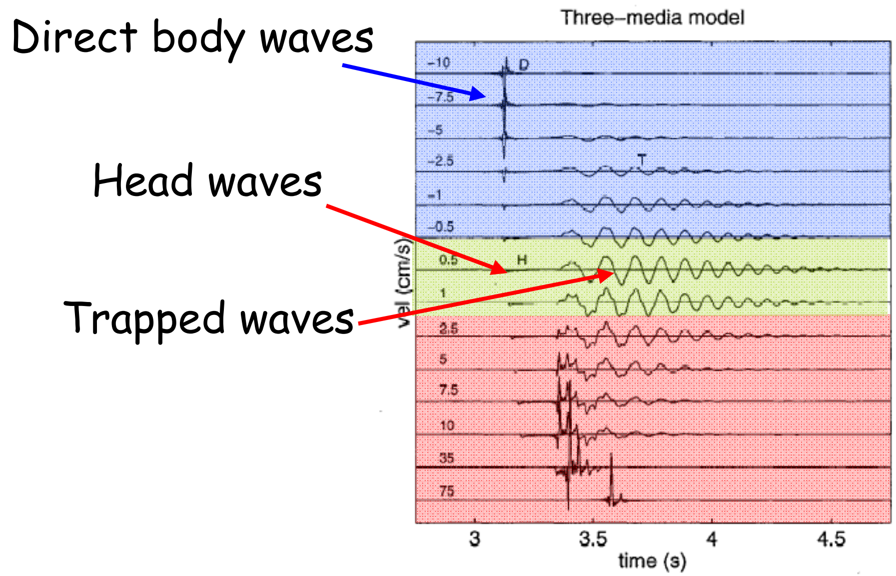

Trapped waves depends strongly on

$$N = r/[W \tan(\theta_c)] = r/[W \tan(\sin^{-1}(\beta_2/\beta_1))]$$

Imaging bimaterial fault interface with Head Waves

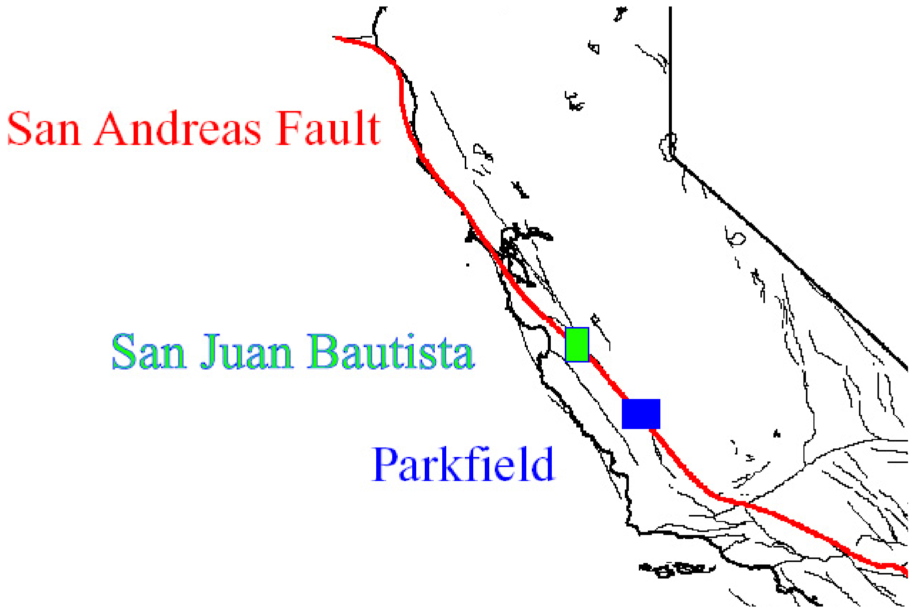

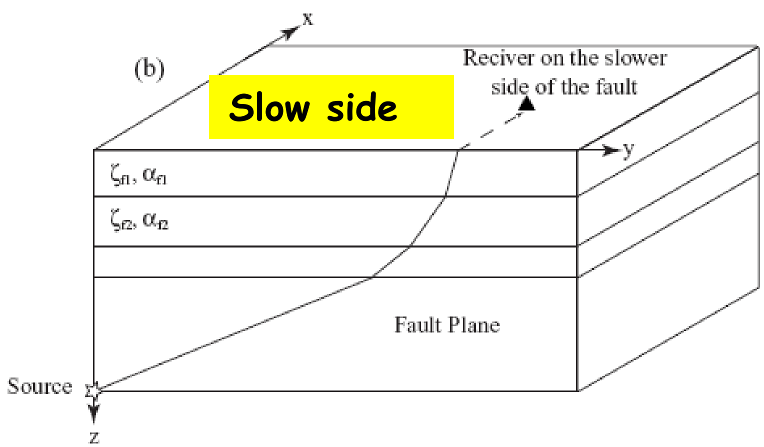

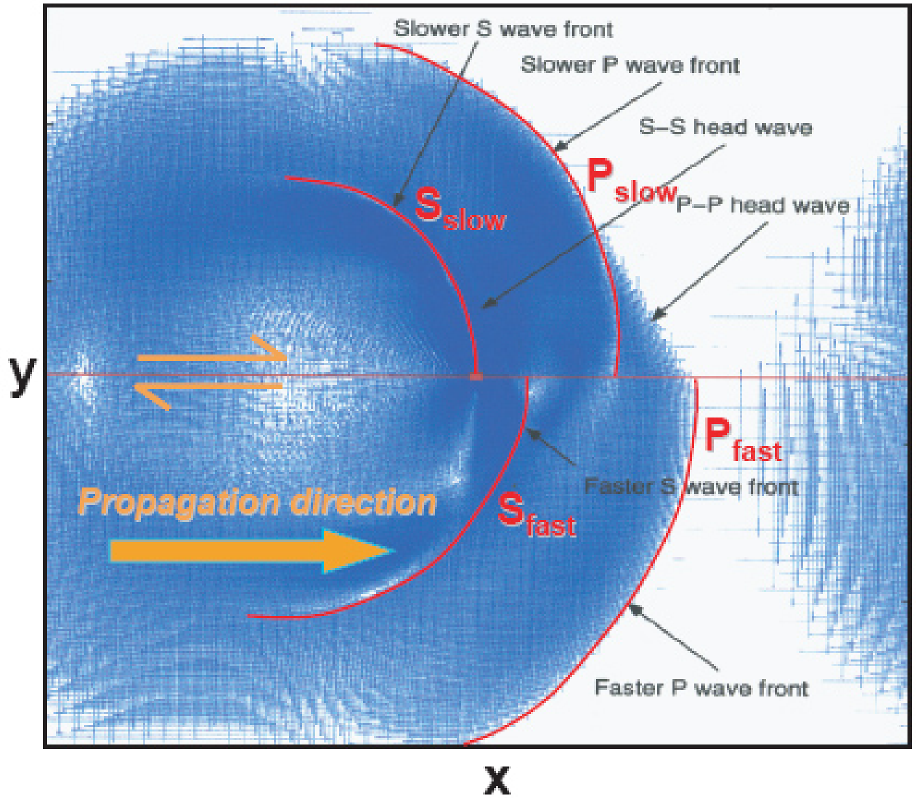

The head waves are first arrivals at stations on the slower side of the fault with normal distance $x < x_c = r \tan[\cos^{-1}(\alpha_2/\alpha_1)]$ and have opposite polarity than the direct *P* wave (Ben-Zion, 1989, 1990)

Fault zone head and trapped waves

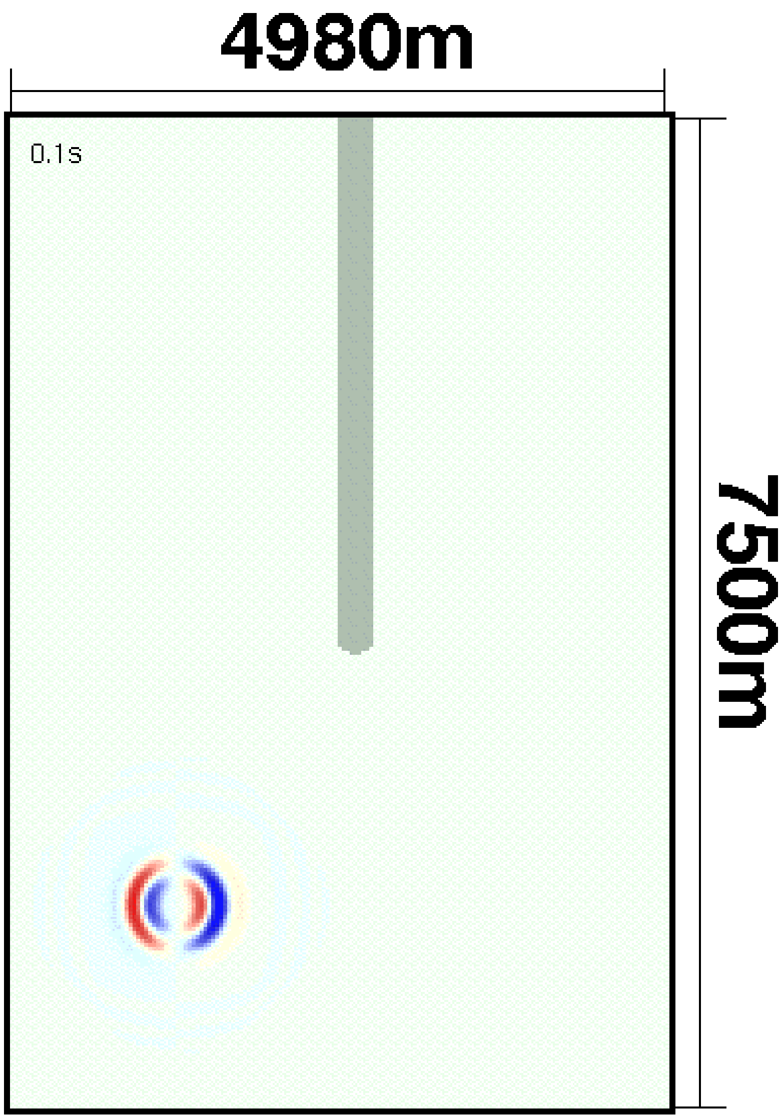

Fohrmann, Igel, Jahnke, Ben-Zion (2004)

Ben-Zion and Aki, 1990

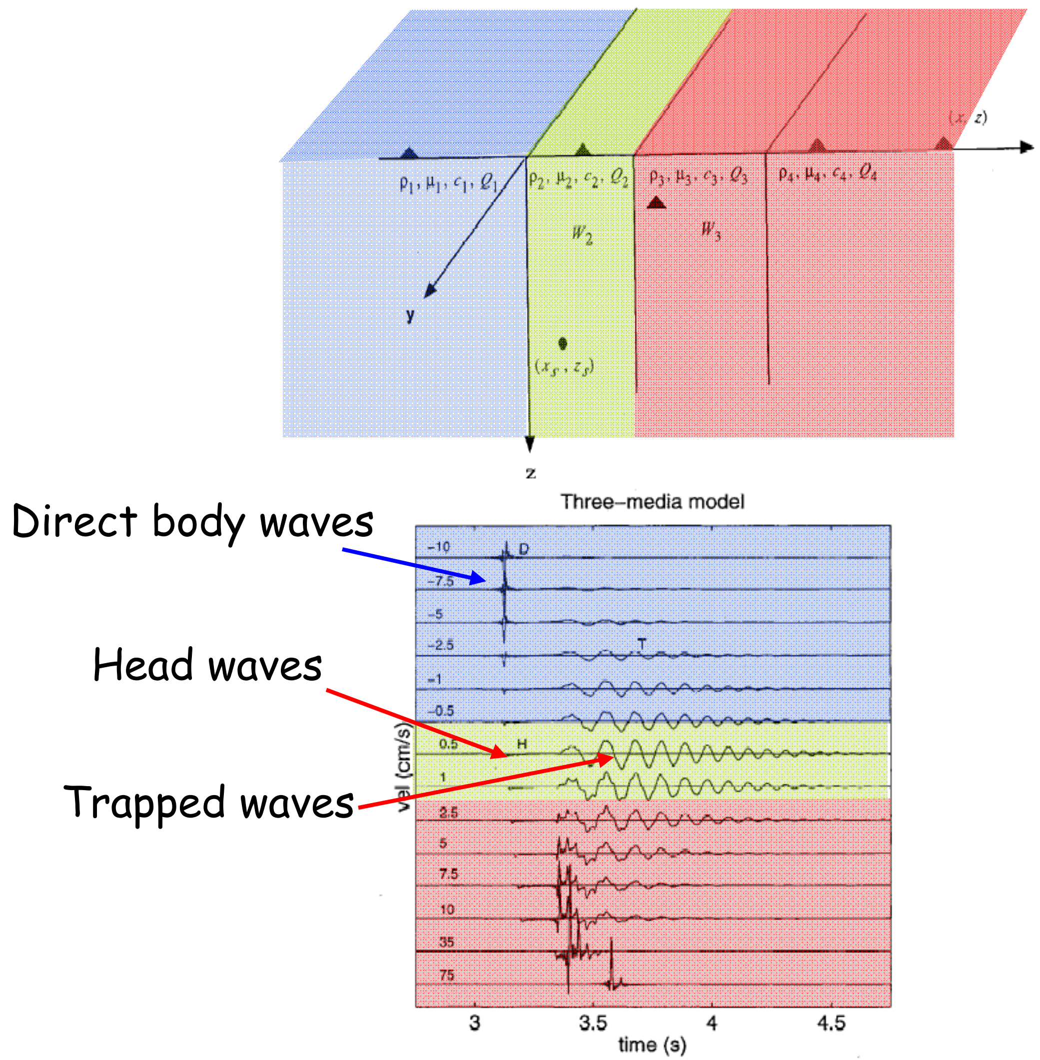

Trapped waves depends strongly on

$N = r/[W \tan(\theta_c)] = r/[W \tan(\sin^{-1}(\beta_2/\beta_1))]$

Internal structure of the San Jacinto fault zone at Jackass Flat (JF) from data recorded by a dense linear array (Qiu, H., Y. Ben-Zion, Z. Ross, P.-E. Share and F. Vernon, 2015)

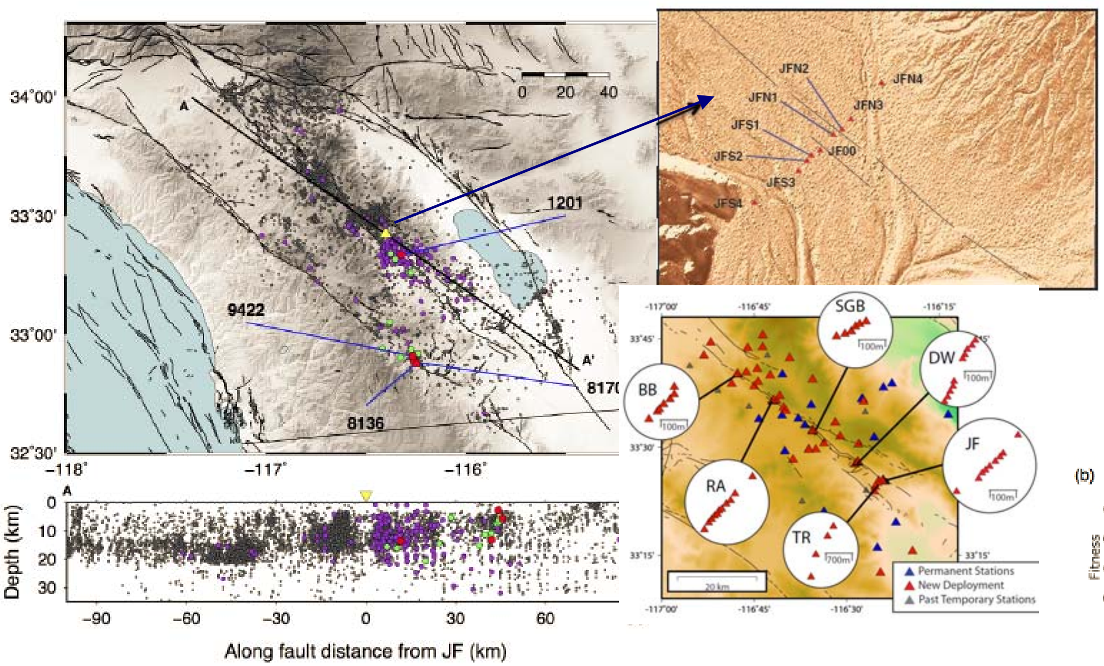

Events generating trapped waves at the JF array (colored circles)

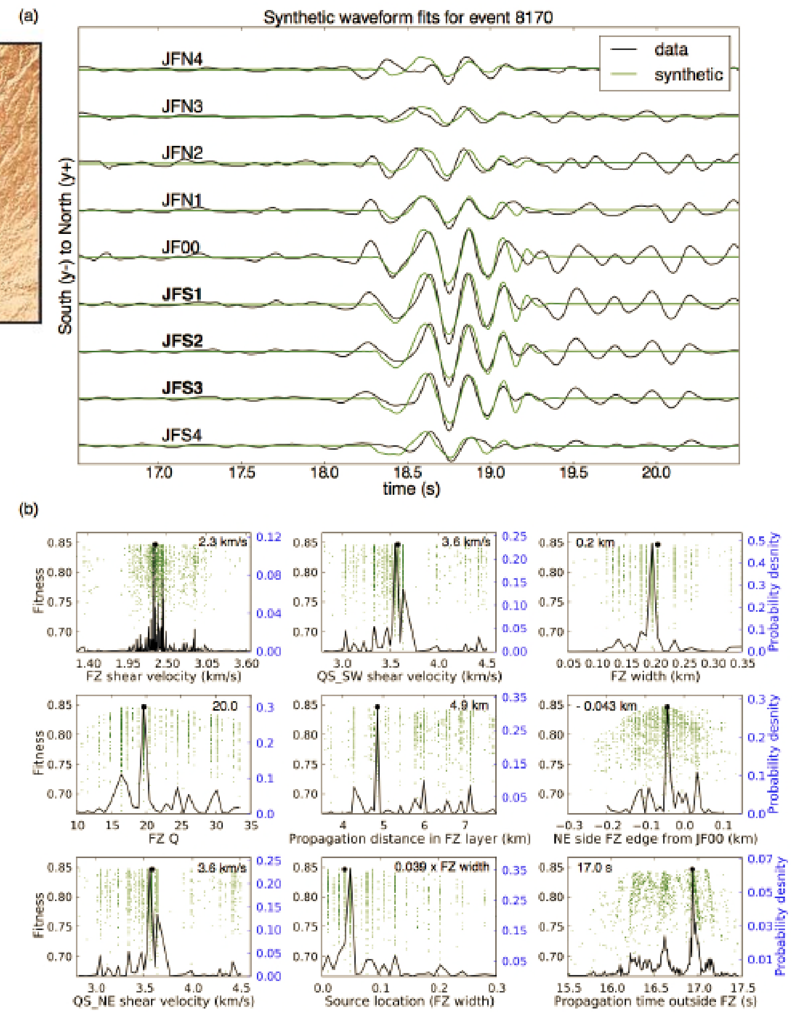

Most likely damage zone parameters:
width ~200 m,
depth ~3.5 km,
S velocity reduction ~50%,
Q-value ~20.

Top: synthetic waveform fits.

Bottom: parameter-space results of genetic inversion algorithm.

Rupture zone of the 1992 Landers, CA, earthquake (Peng et al., *GJI*, 2003)

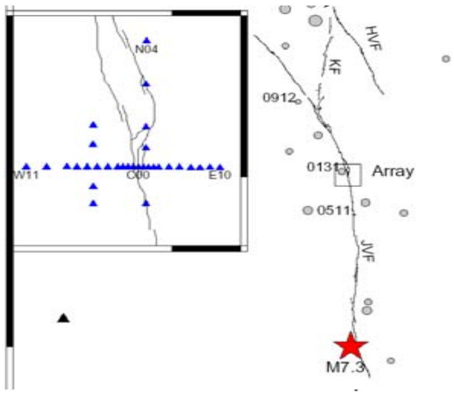

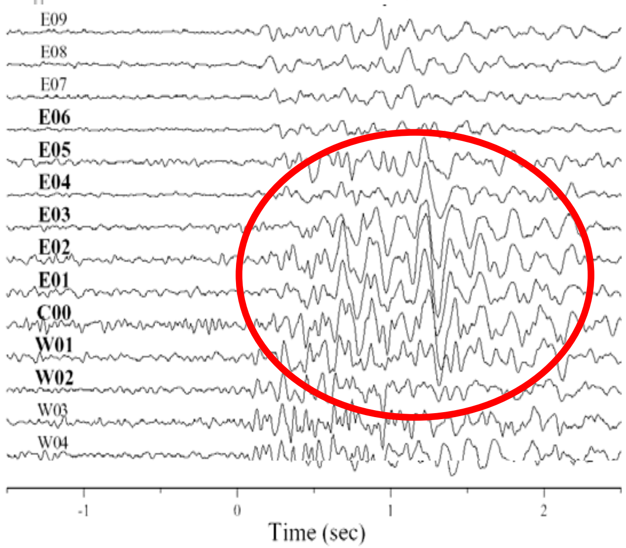

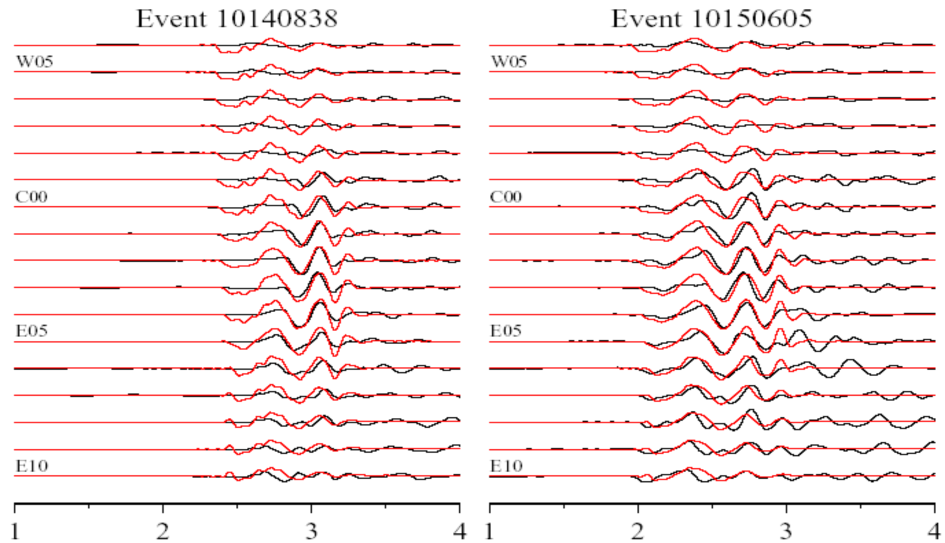

Similar results are obtained from analyses of trapped waves also at the:

Karadere-Duzce branch of the NAF (Ben-Zion et al. 2003)

·**Parkfield section of the San Andreas Fault** (Li et al., 1990; Lewis and Ben-Zion, 2010)

·***Calico fault, ECSZ, CA*** (Yang et al., 2011)

·**Rupture zones of the 1994 Kobe and 2009 L'Aquila events** (e.g., Mizuno & Nishigami 1998; Caldernoni *et al.* 2013)

Most likely damage zone parameters:

width ~200 m,
depth ~3.5 km,
S velocity reduction ~50%,
Q-value ~15.

Detailed analyses of subsets of data imply strong along-strike variations and discontinuities of the trapping structures! (Lewis & Ben-Zion, GJI, 2010)

Trapped noise: paper & poster by G. Hillers et al.

Characterization of the San Jacinto Fault Zone northwest of the trifurcation area from dense linear Black Burn (BB) array data (Share, P.-E., Y. Ben-Zion, Z. Ross, H. Qiu and F. Vernon, 2015)

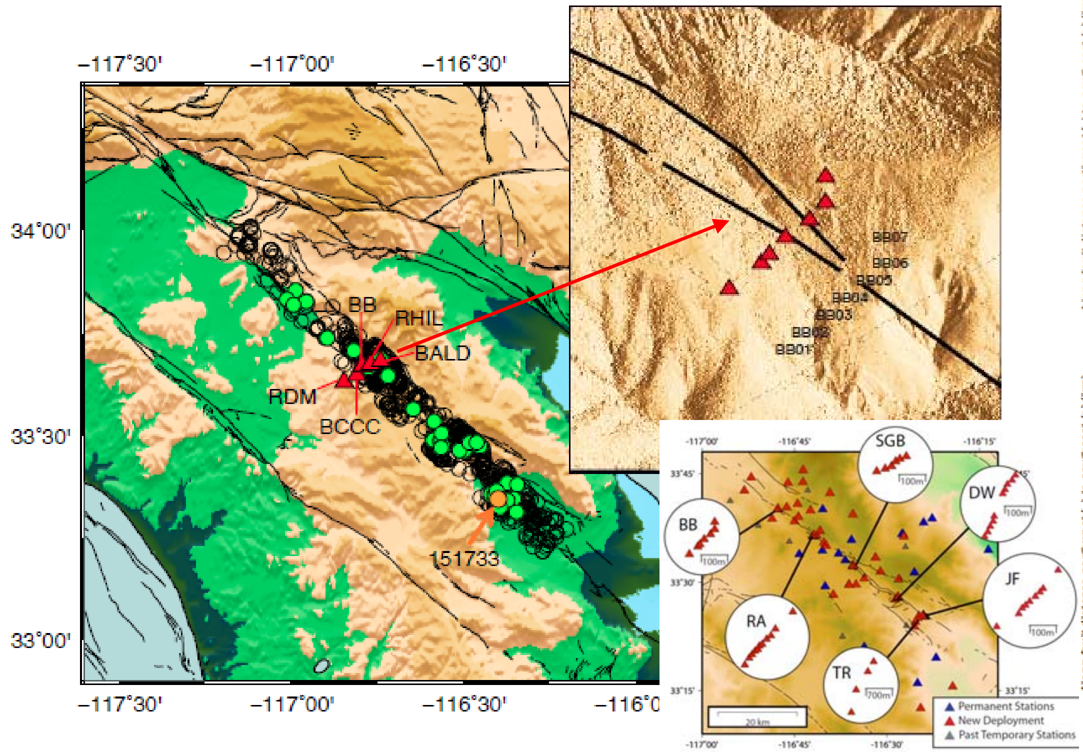

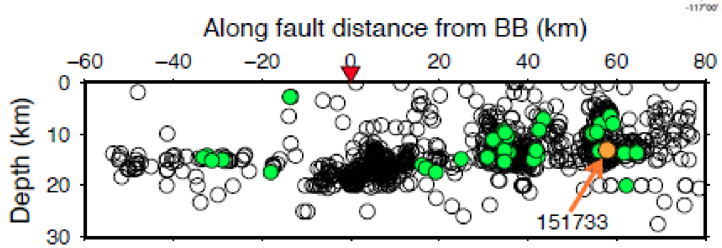

Events generating candidate head waves waves at the BB array (green circles)

Sharp bimaterial interface; average velocity contrast 4-5% over top 15 km
(can be twice as large in the top 7.5-10 km)

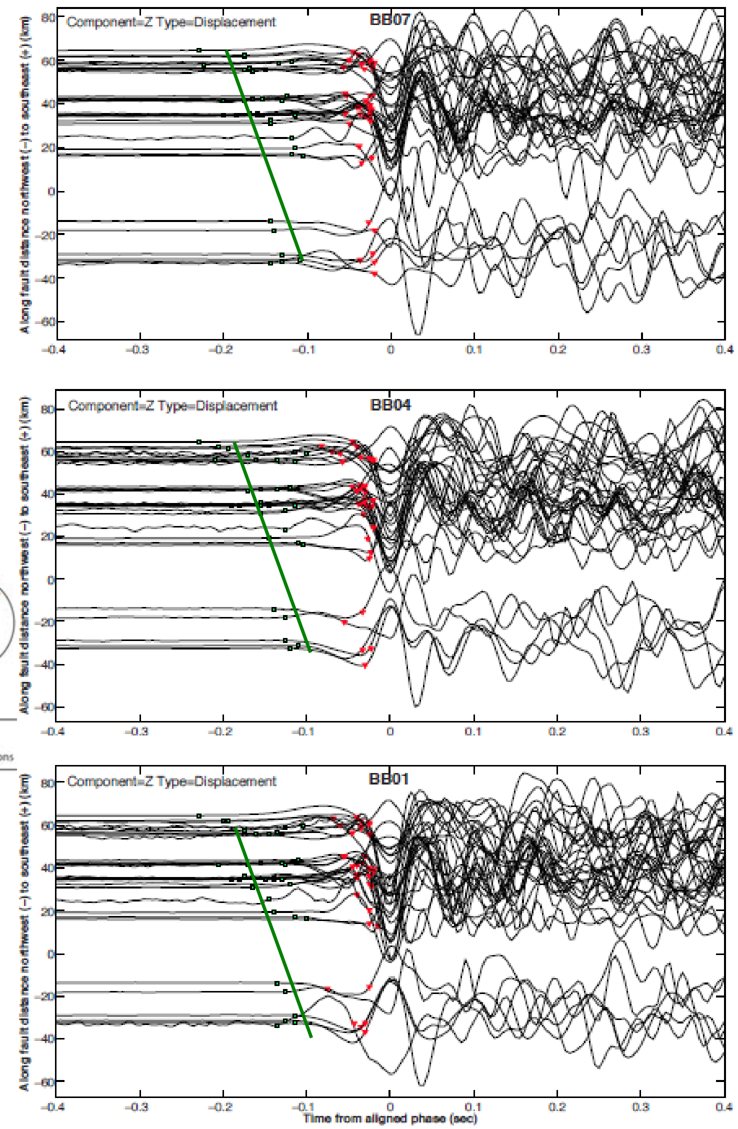

Fault zone head (green) and direct P (red) waves at 3 stations of the BB array from 35 events.

Bimaterial interface along the Hayward fault

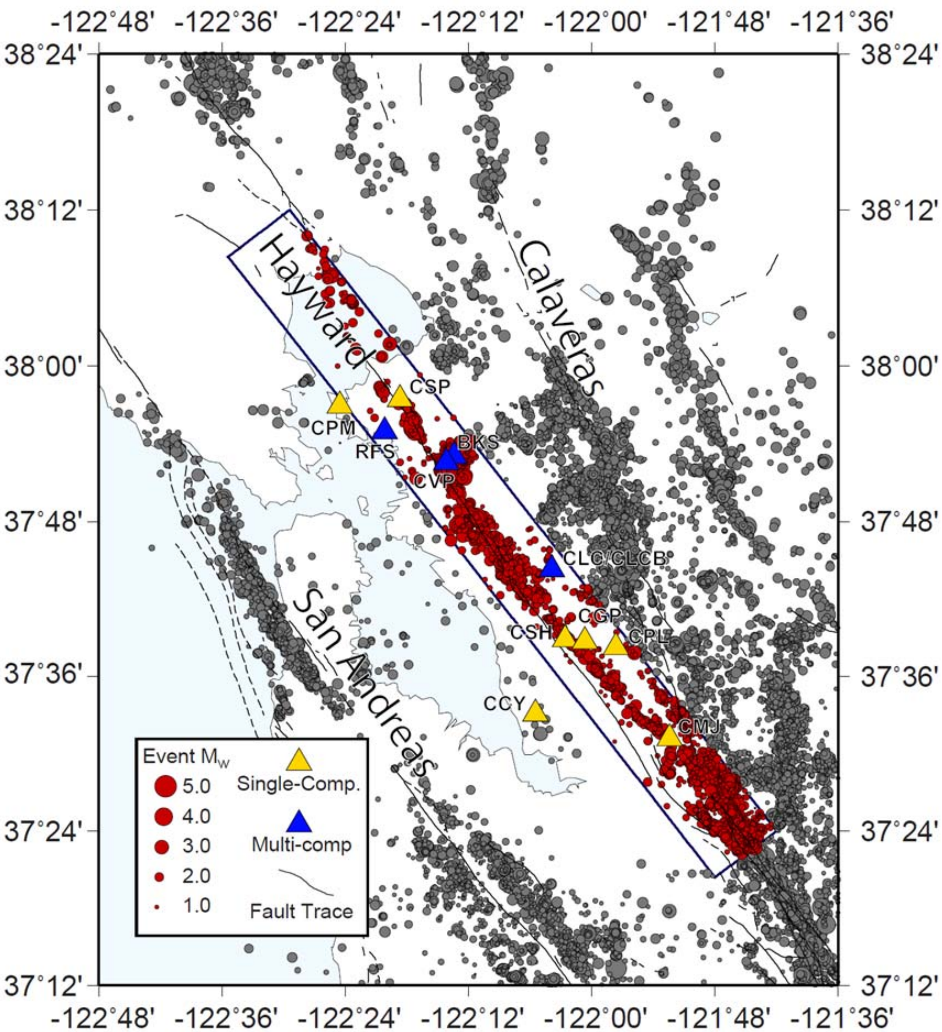

Allam, Ben-Zion & Peng (2014)

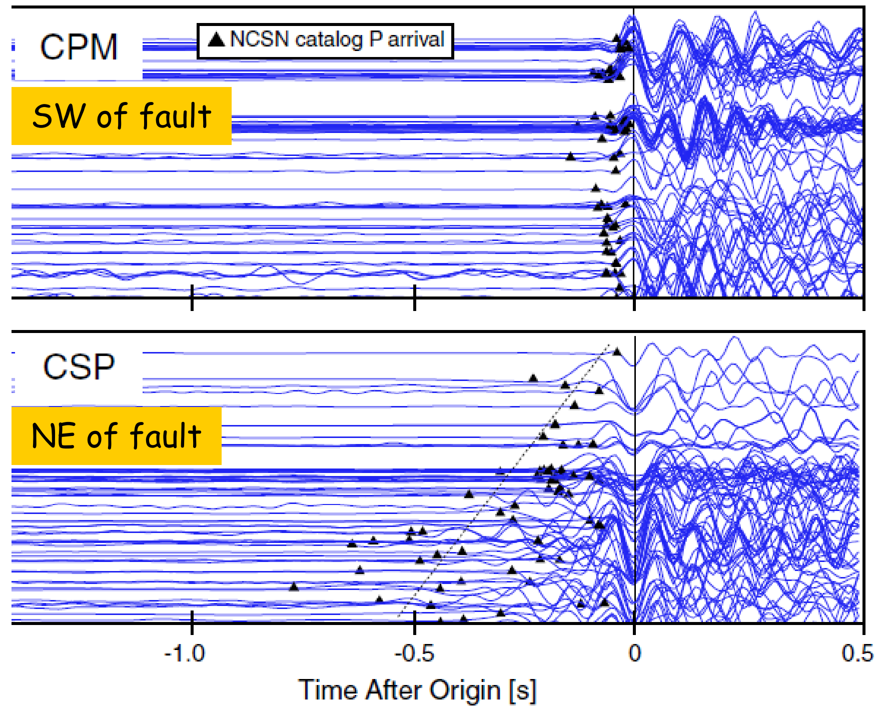

There is a continuous bimaterial interface for ~80km along the Hayward fault with 3-8% velocity contrast

Similar results are obtained from analysis of fault zone head waves also at:

Different sections of the San Andreas fault (Ben-Zion and Malin 1991; McGuire and Ben-Zion 2005)

Calaveras fault (Zhao and Peng 2008)

Different sections of the North Anatolian fault (Bulut et al. *2013; Bita et al. 2015*)

Garze-Yushu fault in Tibet (Yang et al. 2015)

Eastern CA shear zone (Hough et a. 1994)

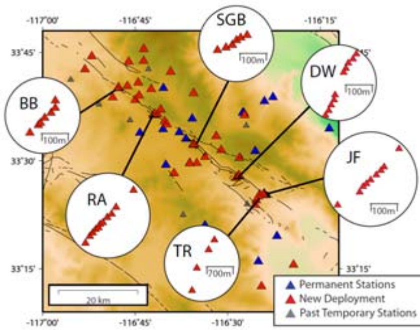

Imaging the top few 100 m with correlations of high-frequency noise across SJFZ array DW

(Zigone, Ben-Zion, Campillo, Hillers, Roux, Vernon, 2015)

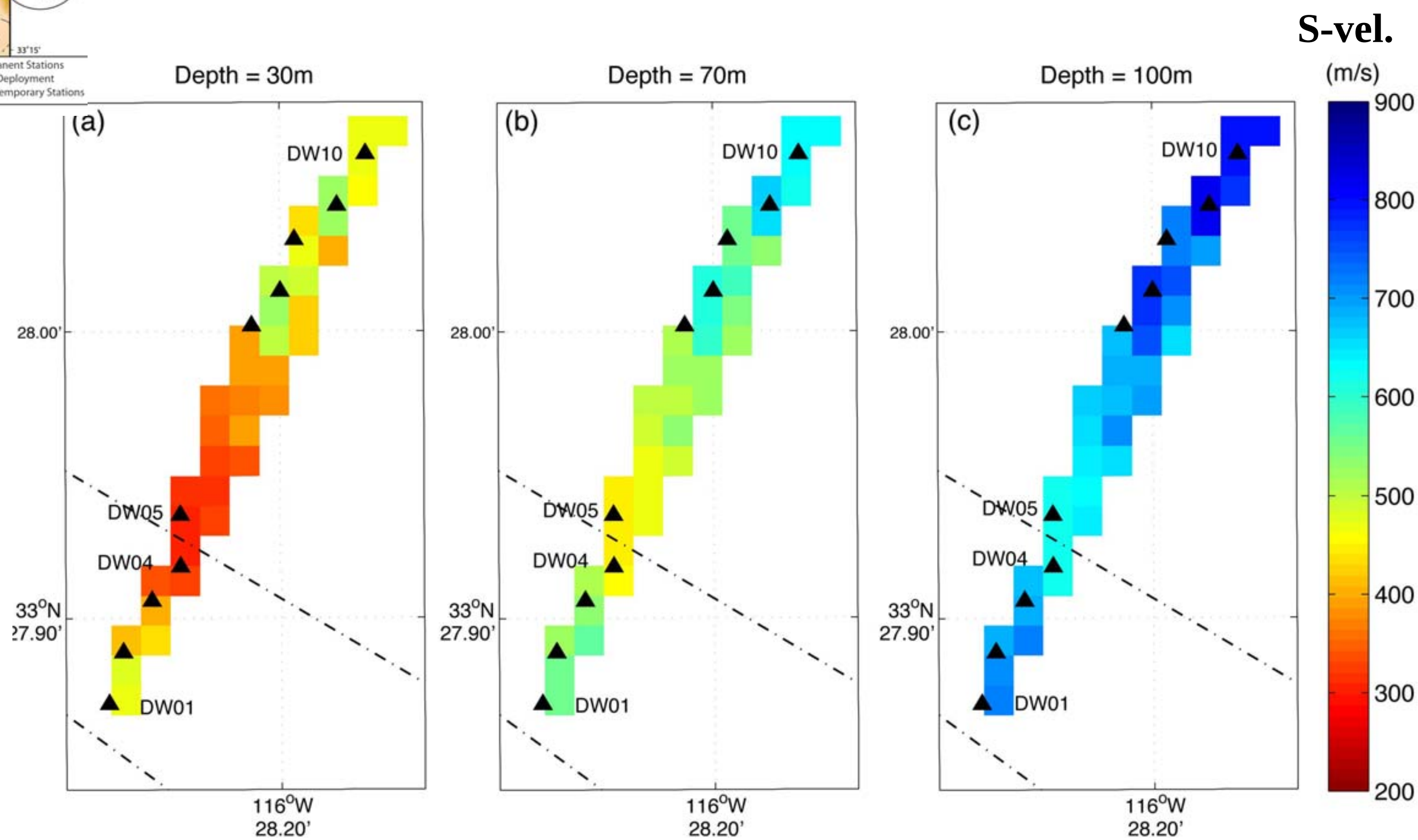

- Low velocity zone around the surface trace of the fault
- Flower structure with depth
- Vs30 ~ 250 m/s similar to borehole observations

poster by D. Zigone et al.

Dense deployment

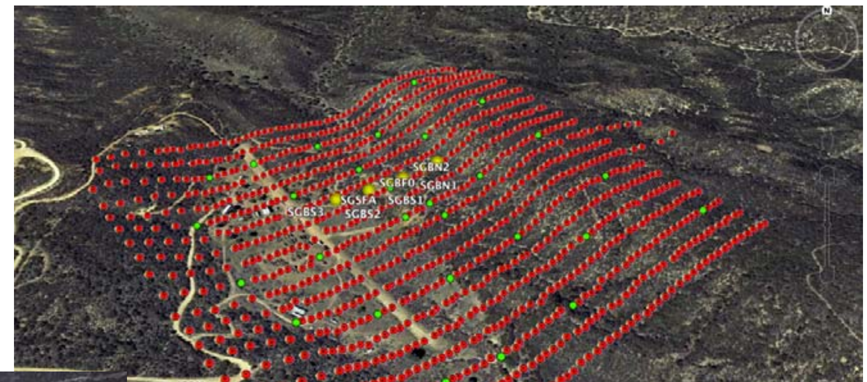

Sage Brush Flats - Clark Fault

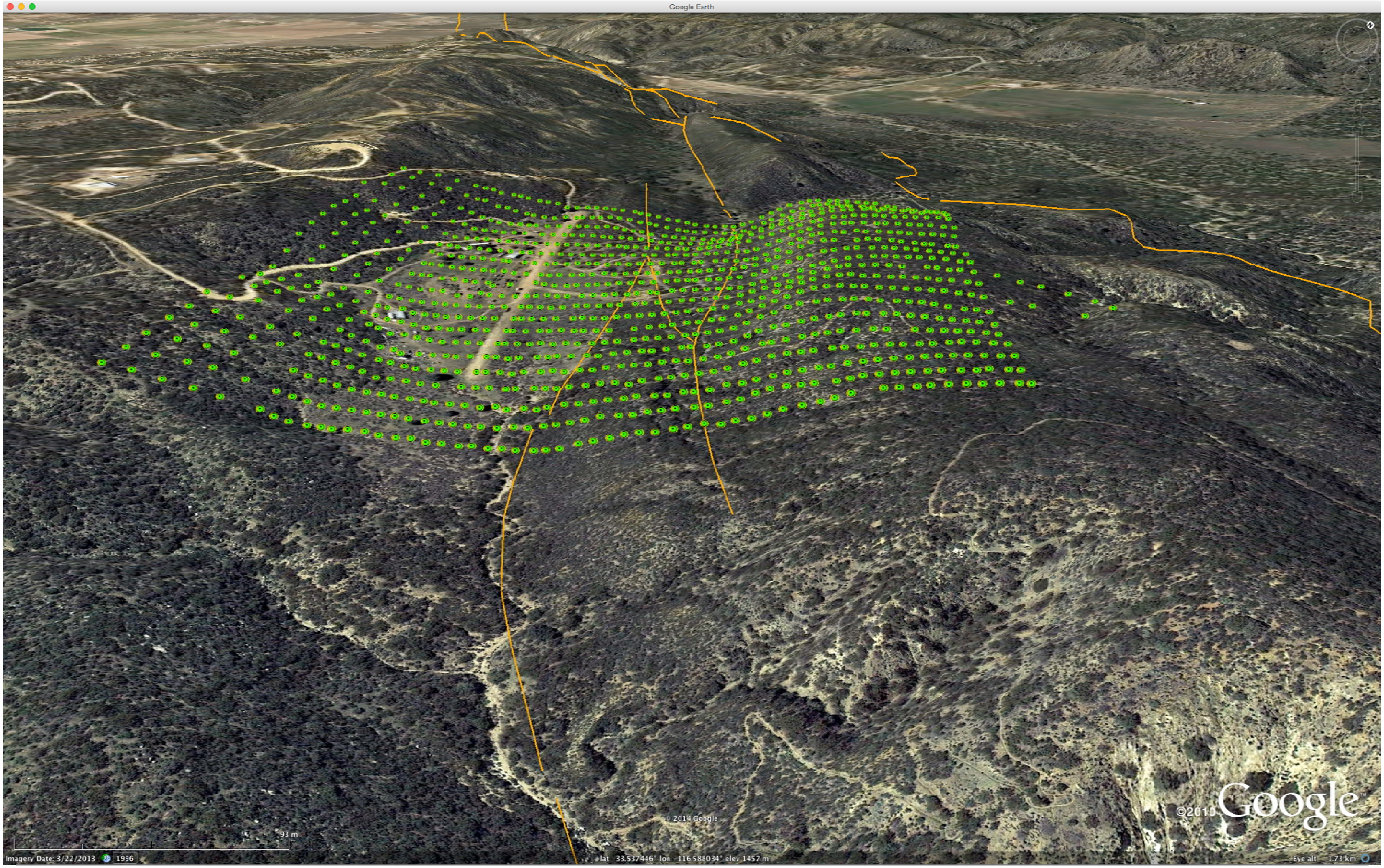

Basic data features and results from a spatially-dense seismic array on the San Jacinto fault zone

Ben-Zion, Vernon, Ozakin, Zigone, Ross, Meng, White, Reyes, Hollis and Barklage (GJI 2015)

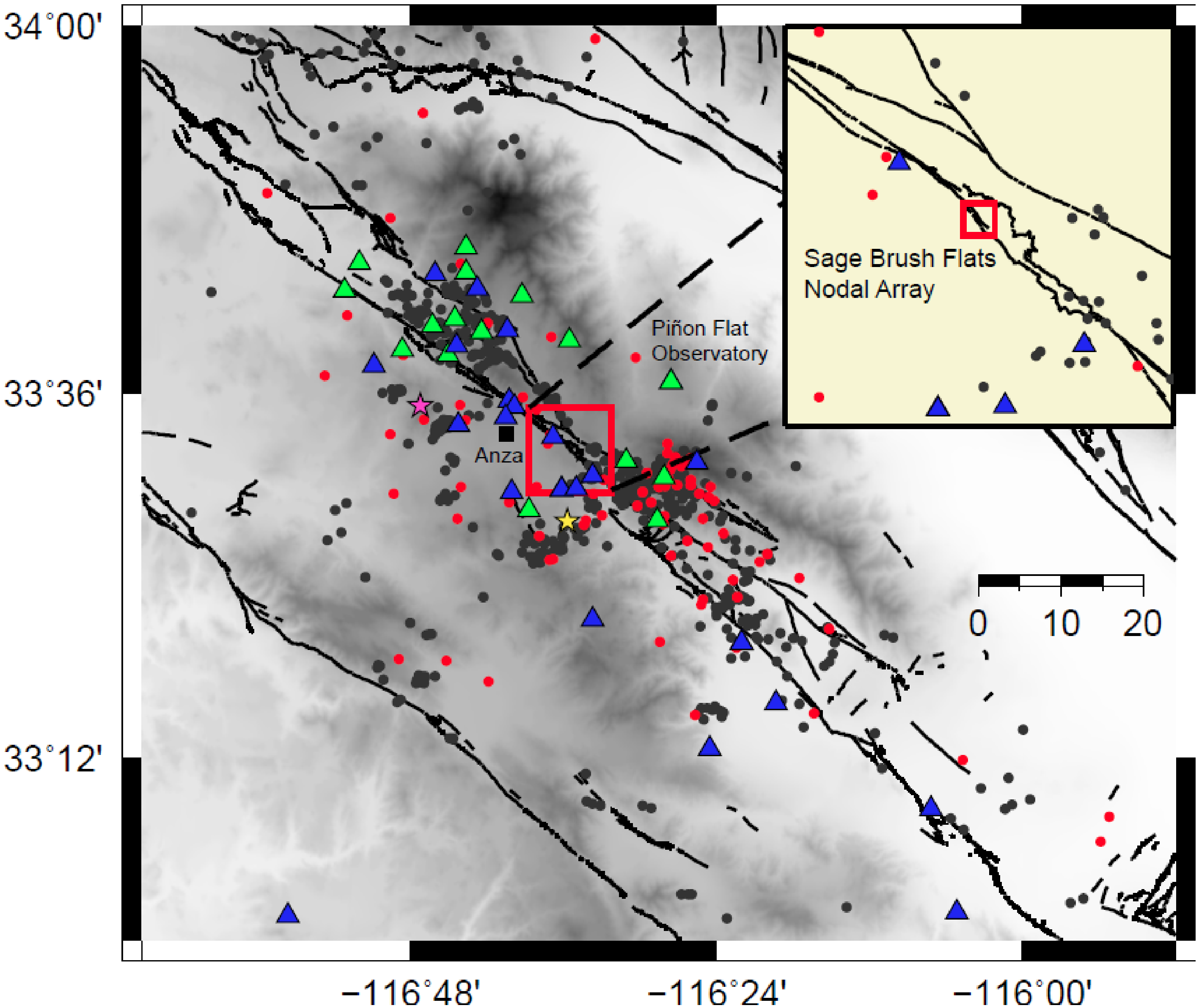

946 events with $-0.7 \leq M_L \leq 3.4$ were detected in the >4 weeks deployment period by the stand-alone stations (black circles)

120 events (90 of which undetected by the ANZA network) with median and minimum size -0.29 and -1.58 were detected in 24 hrs by the dense network (red circles)

Data at 2 stations in Julian day 146

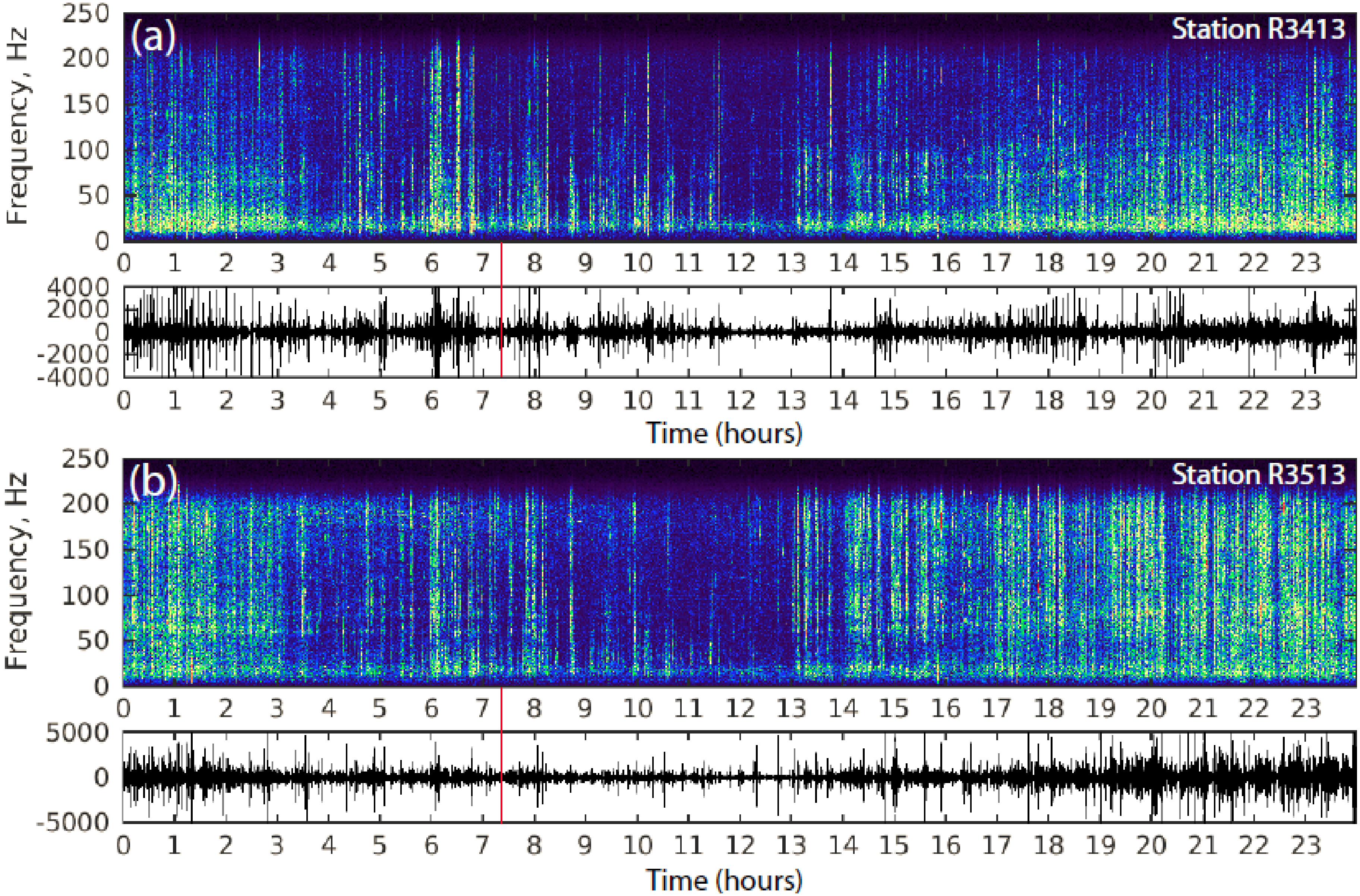

Seismograms from one event (yellow star in map)

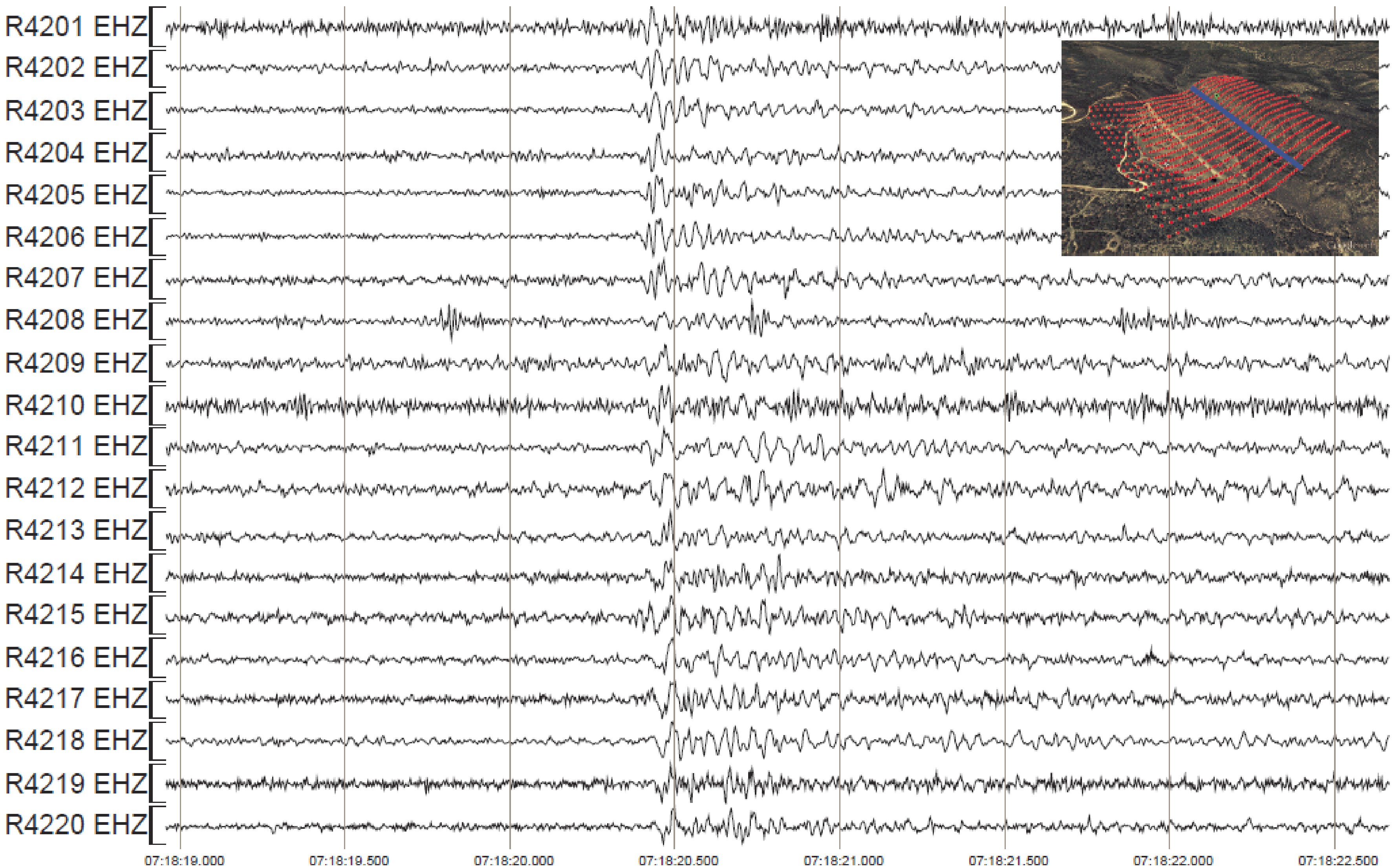

Seismograms from another event (pink star in map)

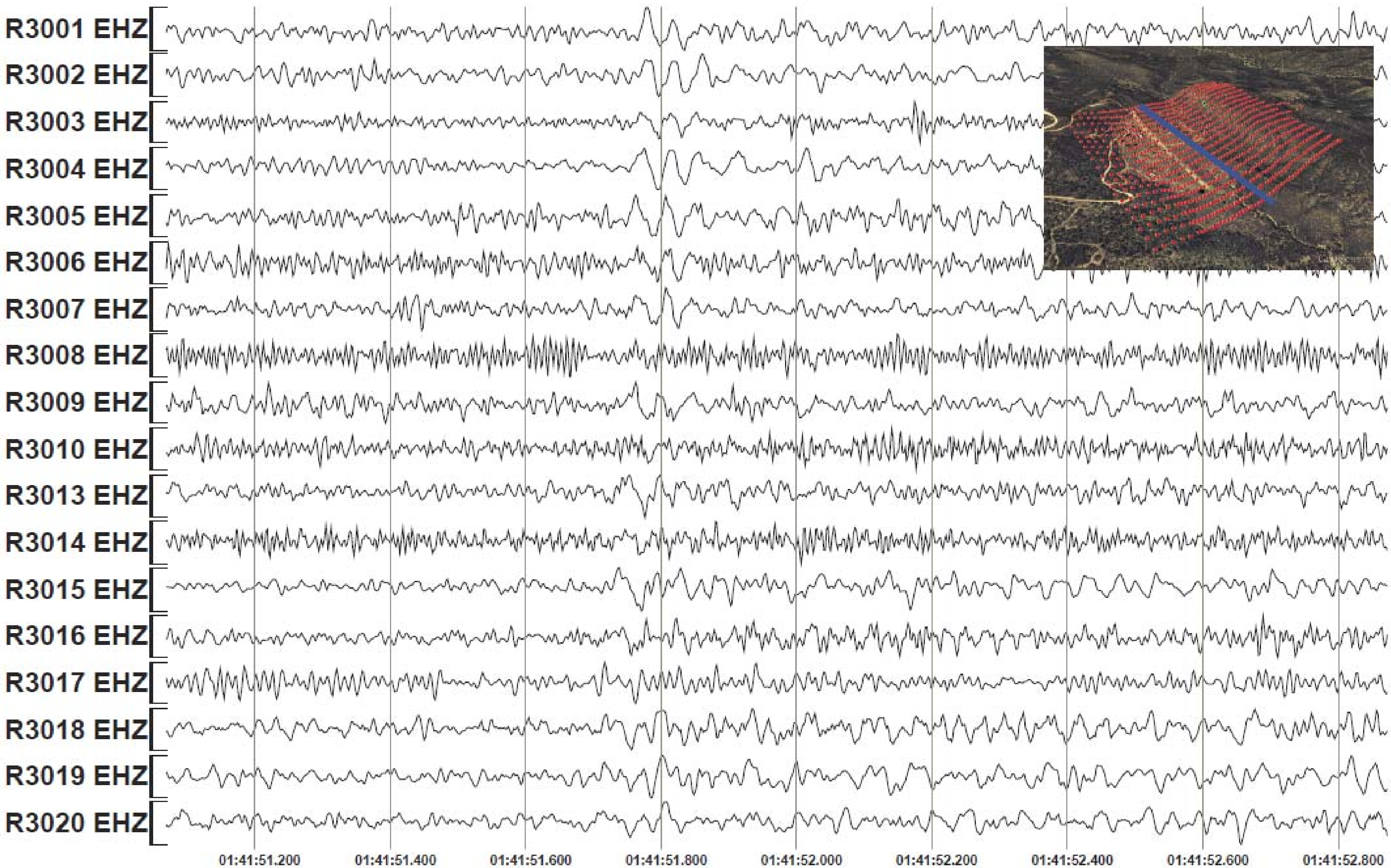

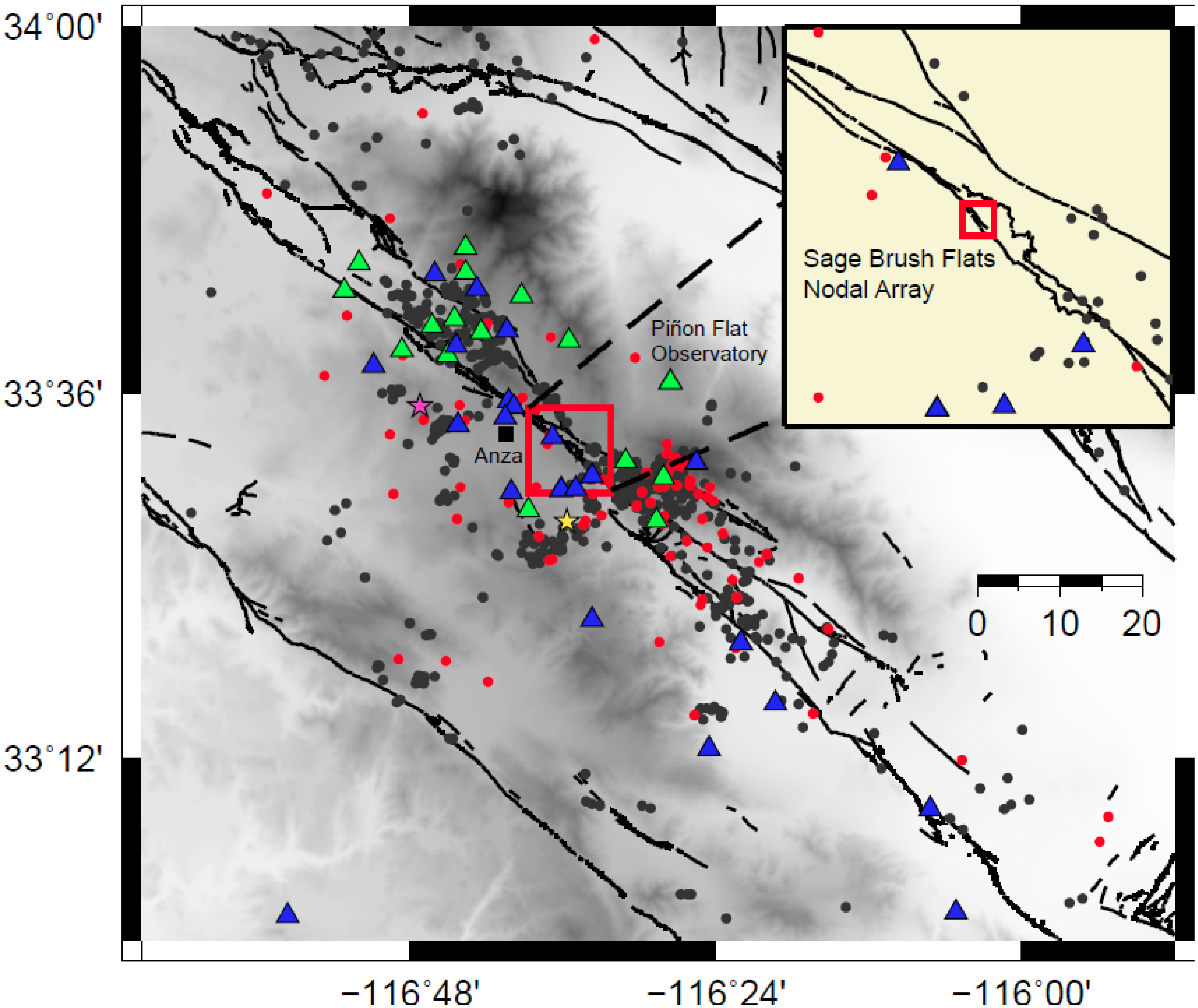

946 events with $-0.7 \leq M_L \leq 3.4$ were detected in the >4 weeks deployment period by the stand-alone stations (black circles)

120 events (90 of which undetected by the ANZA network) with median and minimum size -0.29 and -1.58 were detected in 24 hrs by the dense network (red circles)

Times of 120 events in JD 146: vertical lines

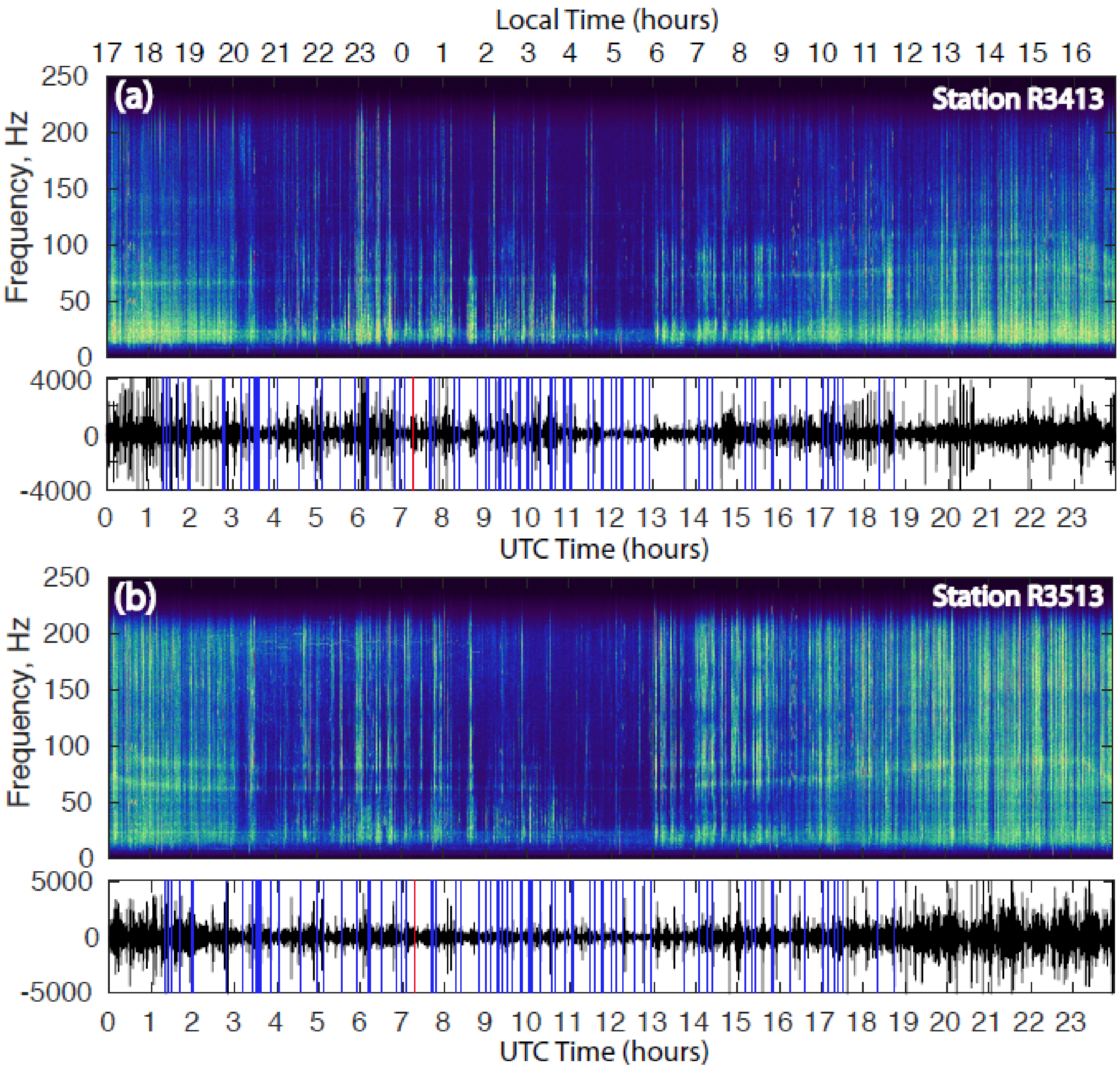

Cross-correlations

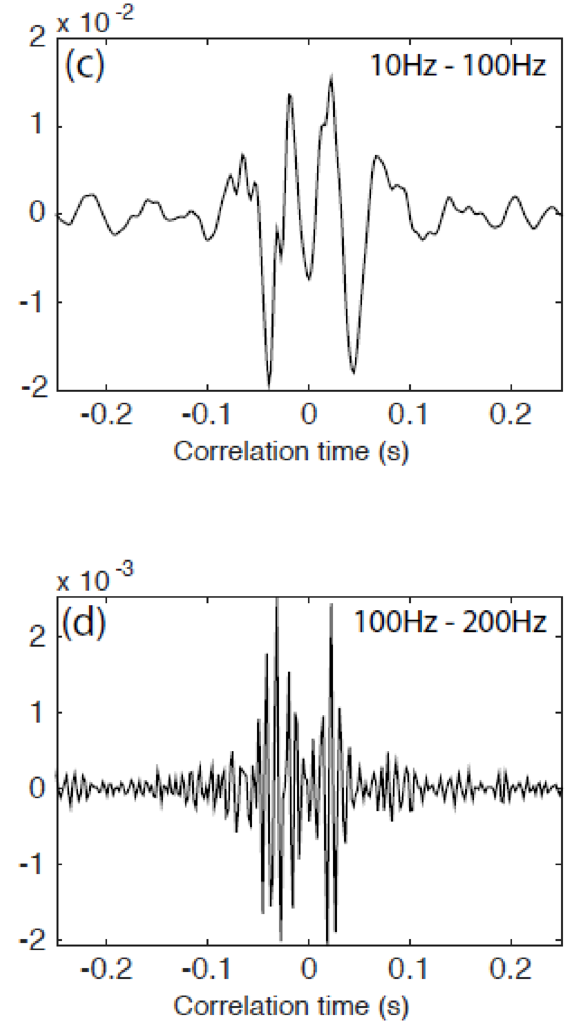

Data at 10-15 Hz are coherent across the entire array

Beamforming analysis of repeating sources in JD 146

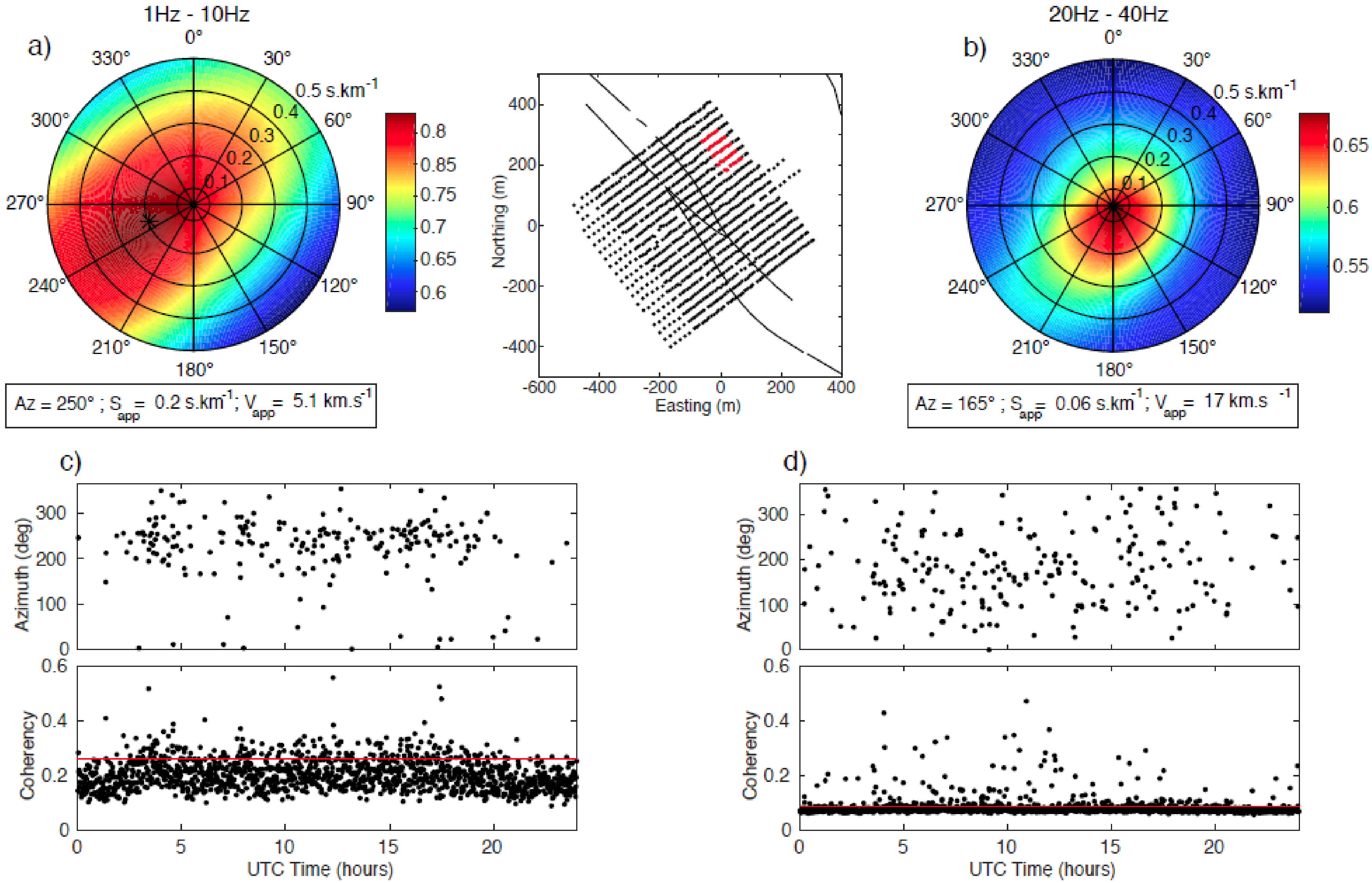

Event location with matched field processing and back projection

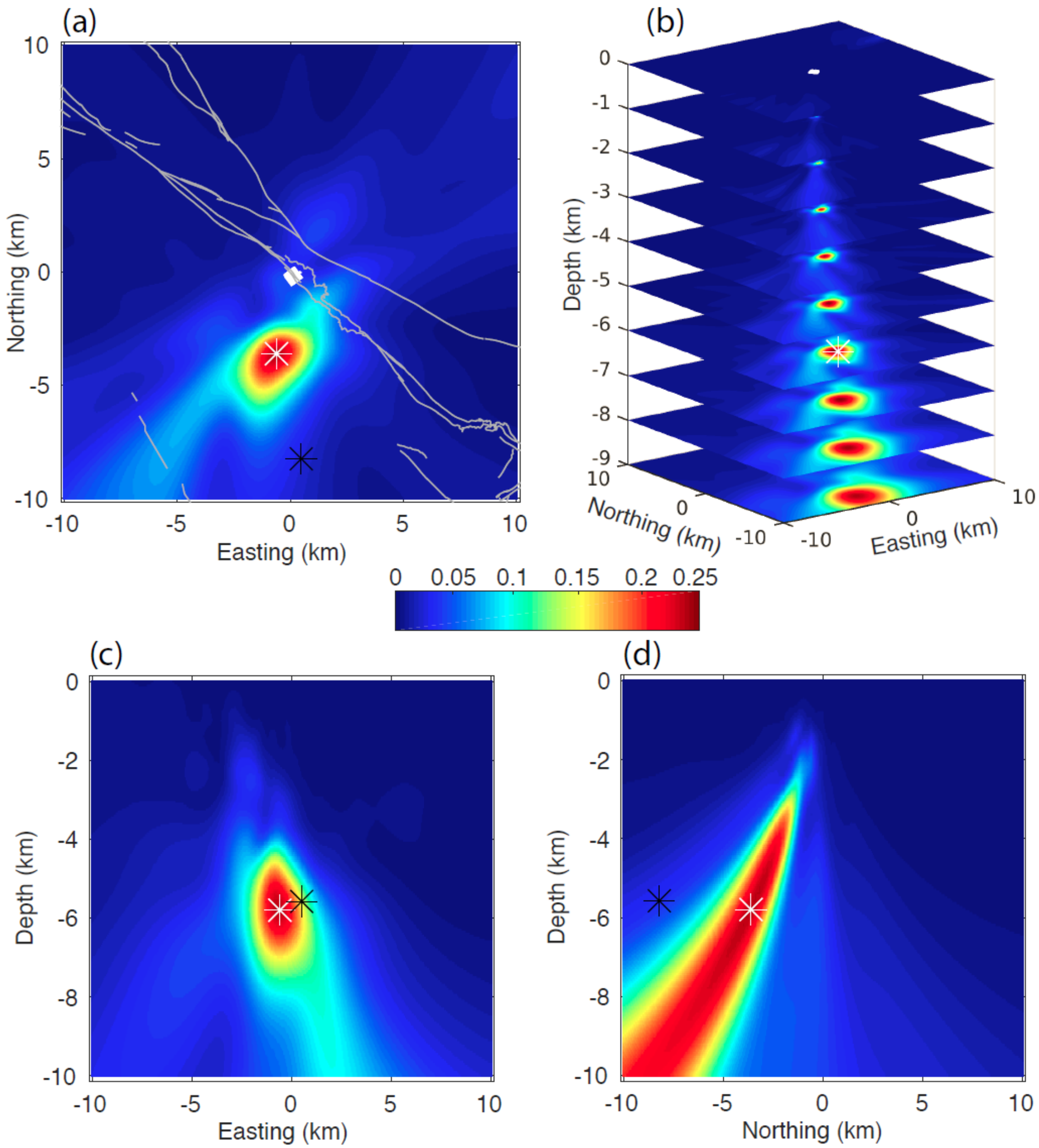

Original location (yellow star in previous plot): **black asterisk**

MFP location: **white asterisk**

Median noise levels during the experiment (note zones with amplified motion)

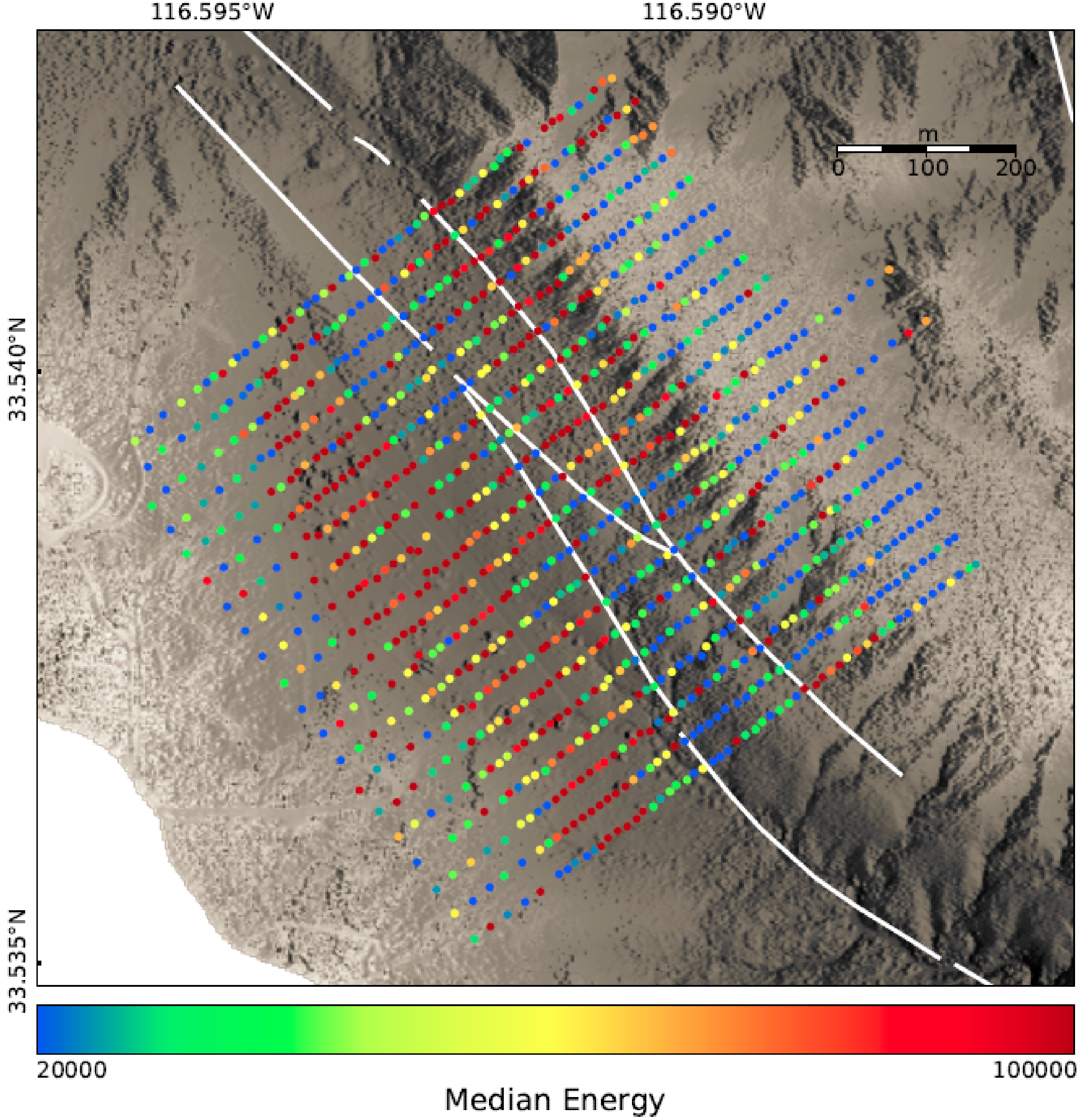

Snapshot of ground motion produced by local earthquake

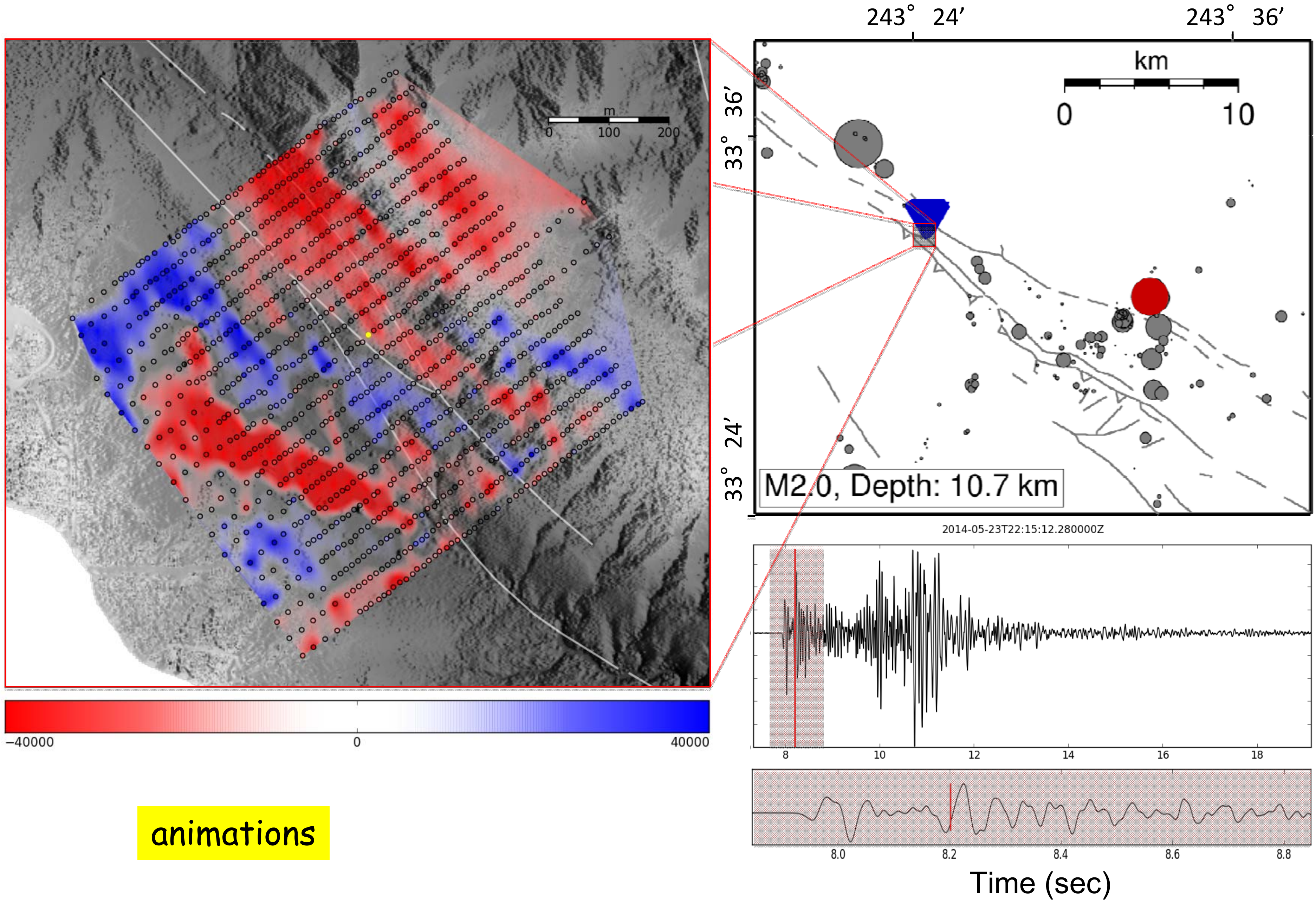

animations

Trapped fault zone waves from Betsy gunshots

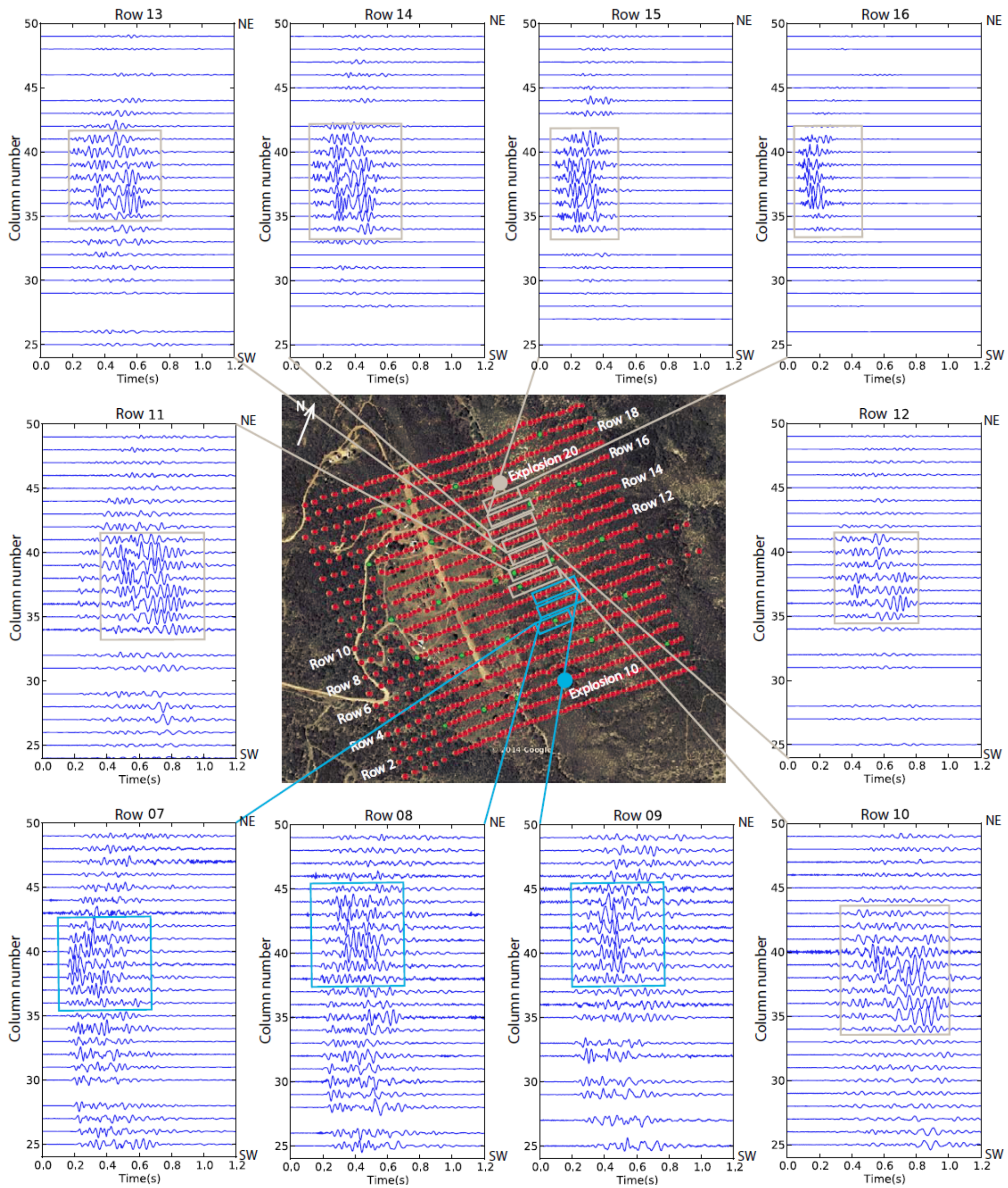

animations

Imaging the shallow material with high-frequency noise in row 13 of the array

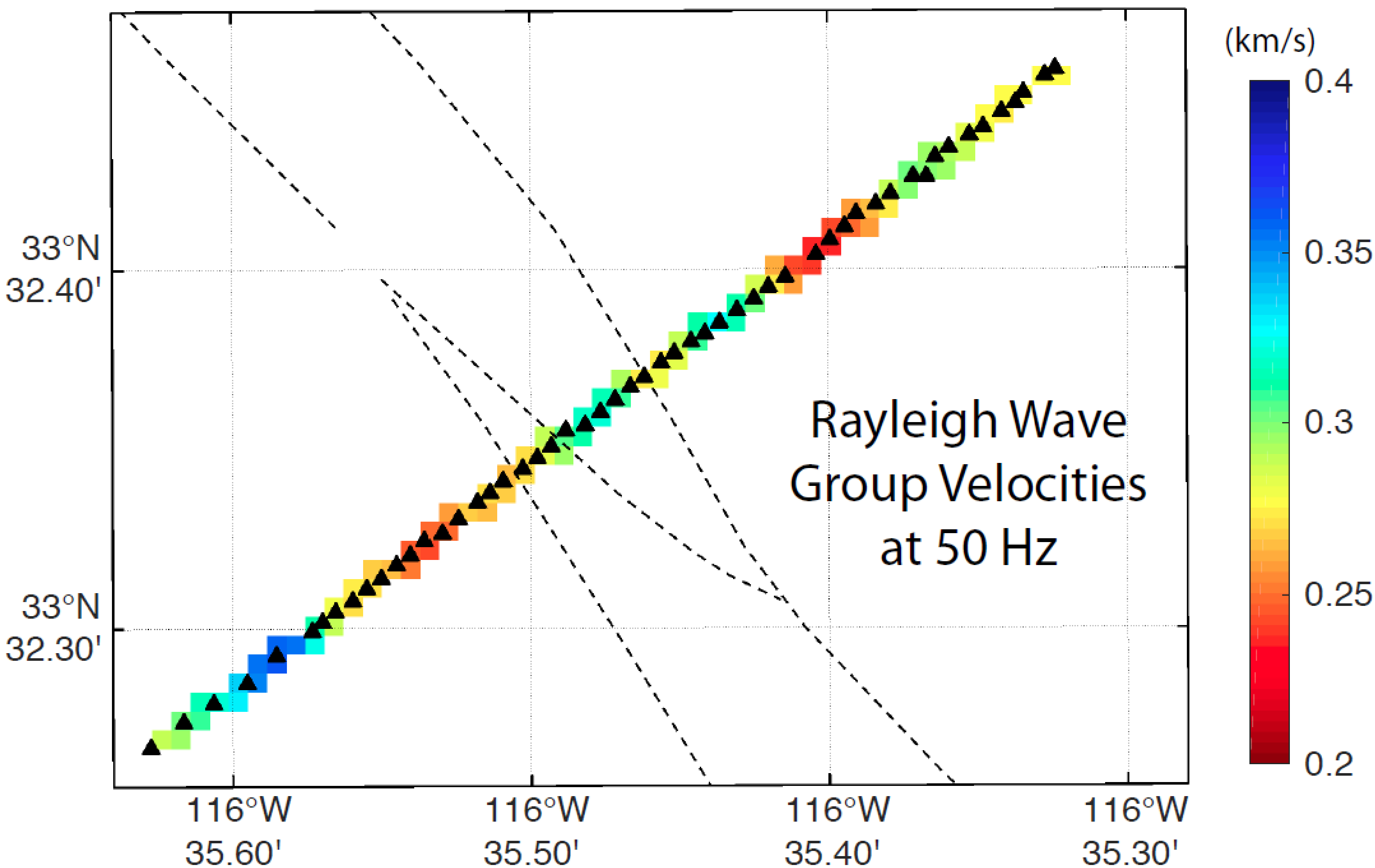

poster by D. Zigone et al.

Conclusions

- High resolution imaging of fault zone environments requires using different signals (body waves, head and trapped waves, scattered waves, anisotropy, surface waves, …) and techniques (travel time and waveform tomography, noise correlations, …).
- Earthquake data provide detailed information on the seismogenic sections (depth 3-15 km).
- Ambient noise data provide detailed information on the shallower structure (up to the surface).

- Large fault zones have hierarchical flower-type damaged zones and bimaterial interfaces.
- The damage zones have ~100m wide cores with intense damage (e.g. $\Delta\beta$ ~ 30-50%, Q ~ 10-30) that act as seismic trapping structures. They have considerable along-strike variability & discontinuities over length scales of ~5 km and are surrounded by ~3-5 km zones of lower damage that produce fault-related anisotropy, elevated scattering and motion amplification.
- Prominent bimaterial interfaces extend to the bottom of the seismogenic zone and are continuous over 10s to 100 km. There are also shallow bimaterial interfaces (e.g. at the edge of damage zones)
- The damage zones get re-activated during earthquakes (strong co-seismic velocity reduction of 30-40 % in the top few 100's of m of the crust) followed by log(t) healing.
- The damage zones are often asymmetric w.r.t. the principle slip zone, which may reflect preferred propagation direction of earthquake ruptures.

Analysis of spatially-dense array:

- Can be used to detect many more smaller quakes
- Locate sources of noise and small quakes
- Study coherency of waves and fine structural details
- The shallow crust sustains numerous ongoing small failures; it is far more dynamic than usually assumed

Thank you